A&A 482, 113–132 (2008)
DOI: 10.1051/0004-6361:20079332

Astronomy & Astrophysics

Unveiling the nature of *INTEGRAL* objects through optical spectroscopy

VI. A multi-observatory identification campaign⋆

N. Masetti[1], E. Mason[2], L. Morelli[3], S. A. Cellone[4,5], V. A. McBride[6], E. Palazzi[1], L. Bassani[1], A. Bazzano[7], A. J. Bird[6], P. A. Charles[6,8], A. J. Dean[6], G. Galaz[9], N. Gehrels[10], R. Landi[1], A. Malizia[1], D. Minniti[9], F. Panessa[7], G. E. Romero[4,11], J. B. Stephen[1], P. Ubertini[7], and R. Walter[12]

[1] INAF – Istituto di Astrofisica Spaziale e Fisica Cosmica di Bologna, via Gobetti 101, 40129 Bologna, Italy
e-mail: masetti@iasfbo.inaf.it
[2] European Southern Observatory, Alonso de Cordova 3107, Vitacura, Santiago, Chile
[3] Dipartimento di Astronomia, Università di Padova, Vicolo dell'Osservatorio 3, 35122 Padua, Italy
[4] Facultad de Ciencias Astronómicas y Geofísicas, Universidad Nacional de La Plata, Paseo del Bosque, B1900FWA La Plata, Argentina
[5] IALP (CONICET–UNLP), Argentina
[6] School of Physics & Astronomy, University of Southampton, Southampton, Hampshire, SO17 1BJ, UK
[7] INAF – Istituto di Astrofisica Spaziale e Fisica Cosmica di Roma, via Fosso del Cavaliere 100, 00133 Rome, Italy
[8] South African Astronomical Observatory, PO Box 9, Observatory 7935, South Africa
[9] Departamento de Astronomía y Astrofísica, Pontificia Universidad Católica de Chile, Casilla 306, Santiago 22, Chile
[10] NASA/Goddard Space Flight Center, Greenbelt, MD 20771, USA
[11] Instituto Argentino de Radioastronomía (CONICET), C.C. 5, 1894 Villa Elisa, Buenos Aires, Argentina
[12] INTEGRAL Science Data Centre, Chemin d'Ecogia 16, 1290 Versoix, Switzerland

Received 27 December 2007 / Accepted 5 February 2008

ABSTRACT

Using 8 telescopes in the northern and southern hemispheres, plus archival data from two on-line sky surveys, we performed a systematic optical spectroscopic study of 39 putative counterparts of unidentified or poorly studied *INTEGRAL* sources in order to determine or at least better assess their nature. This was implemented within the framework of our campaign to reveal the nature of newly-discovered and/or unidentified sources detected by *INTEGRAL*. Our results show that 29 of these objects are active galactic nuclei (13 of which are of Seyfert 1 type, 15 are Seyfert 2 galaxies and one is possibly a BL Lac object) with redshifts between 0.011 and 0.316, 7 are X-ray binaries (5 with high-mass companions and 2 with low-mass secondaries), one is a magnetic cataclysmic variable, one is a symbiotic star and one is possibly an active star. Thus, the large majority (74%) of the identifications in this sample belongs to the AGN class. When possible, the main physical parameters for these hard X-ray sources were also computed using the multiwavelength information available in the literature. These identifications further underscore the importance of *INTEGRAL* in studying the hard X-ray spectra of all classes of X-ray emitting objects, and the effectiveness of a strategy of multi-catalogue cross-correlation plus optical spectroscopy to securely pinpoint the actual nature of still unidentified hard X-ray sources.

Key words. galaxies: Seyfert – X-rays: binaries – stars: novae, cataclysmic variables – techniques: spectroscopic – X-rays: general

1. Introduction

One of the main objectives of the *INTEGRAL* mission (Winkler et al. 2003) is to survey the whole sky in the hard X-ray band above 20 keV. This makes use of the unique imaging capability of the IBIS instrument (Ubertini et al. 2003) which allows the detection of sources at the mCrab level with a typical localization accuracy of 2–3 arcmin (Gros et al. 2003).

The IBIS survey allowed pinpointing, for the first time, extragalactic sources in the so-called "Zone of Avoidance", which hampers observations in soft X-rays along the Galactic plane due to the presence of gas and dust. Moreover, this survey is expanding our knowledge about Galactic X-ray binaries, by showing the existence of a new class of heavily absorbed supergiant massive X-ray binaries (e.g., Walter et al. 2004), by allowing the discovery of supergiant fast X-ray transients (e.g., Sguera et al. 2006; Leyder et al. 2007), by doubling the number of known high-mass X-ray binaries (HMXBs; see Walter 2007), and by detecting a number of new magnetic cataclysmic variables (CVs; e.g., Barlow et al. 2006; Bonnet-Bidaud et al. 2007).

Up to now, IBIS detected more than 500 sources in the hard X-rays between 20 and 100 keV (see e.g., Bird et al. 2007;

⋆ Based on observations collected at the following observatories: ESO (La Silla, Chile), partly under program 079.A-0171(A); Astronomical Observatory of Bologna in Loiano (Italy); Astronomical Observatory of Asiago (Italy); Cerro Tololo Interamerican Observatory (Chile); Complejo Astronómico El Leoncito (San Juan, Argentina); South African Astronomical Observatory (Sutherland, South Africa); Observatorio del Roque de los Muchachos of the Instituto de Astrofísica de Canarias (Canary Islands, Spain); Anglo-Australian Observatory (Siding Spring, Australia); Apache Point Observatory (New Mexico, USA).

Krivonos et al. 2007; see also Bodaghee et al. 2007). Most of these sources are known Galactic X-ray binaries (∼35% of the total number of detected objects), followed by active galactic nuclei (AGNs, ∼28%) and CVs (∼5%). However, a large number of the remaining objects (about 27% of all the IBIS detections) has no obvious counterpart at other wavelengths and therefore cannot immediately be associated with any known class of high-energy emitting objects. The multiwavelength study of these unidentified sources is thus critical to determine their nature. Therefore, in 2004 we started a multisite observational campaign devoted to the identification of these unidentified objects through optical spectroscopy (see Masetti et al. 2004, 2006a,b,c,d; hereafter Papers I–V). Our results showed that about half of these objects are nearby ($z \lesssim 0.1$) AGNs (Papers I–V), while a non-negligible fraction (∼15%) of objects belongs to the class of magnetic CVs (Paper V and references therein).

In parallel, as a service to the scientific community, we maintain a web page[1] reporting information on *INTEGRAL* sources identified via optical or near-infrared observations.

Continuing our effort to identify unknown *INTEGRAL* sources, we here present optical spectroscopy of 39 more objects which were detected by IBIS but are still unidentified, unclassified or poorly studied. Their spectra have been obtained at eight different telescopes around the world or retrieved from two public spectroscopic archives.

The paper is structured as follows: in Sect. 2 we explain the criteria used to select the sample of *INTEGRAL* and optical objects for the present observational campaign. In Sect. 3 a description of the observations and of the employed telescopes is given. Section 4 reports and discusses the results, divided into four broad classes of sources (CVs, X-ray binaries, AGNs and peculiar sources), together with a statistical outline of the identifications of *INTEGRAL* sources obtained until now. Conclusions are drawn in Sect. 5.

2. Sample selection

In order to continue our program (Papers I–V) of identification of the *INTEGRAL* sources with unknown or poorly known nature, we first collected all unidentified or unclassified objects belonging to the 3rd IBIS Survey (Bird et al. 2007), the IBIS All-Sky Survey (Krivonos et al. 2007), and the Galactic Center Survey (Revnivtsev et al. 2004a). Further information on some of these sources can be found in Kuiper et al. (2006) and Keek et al. (2006).

We then cross-correlated the IBIS positions with those in the catalogues of soft (<10 keV) X-ray sources. This allowed to reduce the X-ray error box size to typically less than ≲10 arcsec. More specifically, for the present sample, we selected *INTEGRAL* objects which have, within their IBIS error box, single source detections by either *ROSAT* (Voges et al. 1999), or *Swift*/XRT (http://www.asdc.asi.it; see also Landi et al. 2007b,c,d,f; and Rodriguez et al. 2008), or *Chandra* (http://cxc.harvard.edu), or *XMM-Newton* (http://heasarc.gsfc.nasa.gov; see also Saxton et al. 2008; and Walter et al. 2006). This approach was chosen as Stephen et al. (2005, 2006) showed, from statistical considerations, that these are very likely the soft X-ray counterparts of the *INTEGRAL* sources. Indeed, our previous observations, which were based on the same selection criteria, have sucessfully identified 40 selected targets (see Papers I–V).

For the cross-correlation searches, we adopted 90% confidence level *INTEGRAL*/IBIS error circles. This corresponds to error box radii of 3.′5 and 5′ for the IBIS All-Sky Survey (Krivonos et al. 2007) and the Galactic Center Survey (Revnivtsev et al. 2004a), respectively. For the 3rd IBIS Survey sources we adopted the error box radii reported by Bird et al. (2007).

After this first selection of objects with arcsec-sized X-ray positions, we next chose out of them a subsample of cases for which, when these refined error boxes were overlaid onto the corresponding DSS-II-Red survey[2] images, they were found to contain a single or few (3 at most) possible optical counterparts with magnitudes $R \lesssim 20$, that is, objects for which optical spectroscopy could be obtained with reasonable S/N ratio at telescopes of small and medium size (up to 4 m).

In this way we selected 35 sources. However, we note that, for object IGR J08023−6954, we found only a marginal (<3σ) *Swift*/XRT detection within the IBIS error circle, positionally consistent with one putative optical counterpart. For IGR J12131+0700, instead, two *Swift*/XRT soft X-ray sources were found within the IBIS error circle (Landi et al. 2007e). Here, we focus only on the XRT source #1 (according to the notation of Landi et al. 2007e) given that it is the brightest one and it has an optical counterpart.

Three additional sources (IGR J06292+4858, IGR J07437−5137 and IGR J14561−3738) were added to our sample though they do not have a soft X-ray counterpart. The latter two cases were chosen because the IBIS error circle encompasses a single radio source reported in the NVSS (Condon et al. 1998) or SUMSS (Mauch et al. 2003) catalogues, as well as a far-infrared IRAS source (IRAS 1988) consistent with the radio position, and in addition a single optical object could be found at the far-infrared and radio locations. For IGR J06292+4858, instead, we chose a conspicuous optical galaxy within the *INTEGRAL* error box. We in any case refer the reader to Paper III for the caveats and the shortcomings of choosing, within the IBIS error box, "peculiar" sources which are not readily associated with an arcsec-sized soft X-ray position.

A further caveat that is to be mentioned is that some sources of our sample and extracted from the catalogue of Bird et al. (2007), namely IGR J06292+4858, IGR J12131+0700, IGR J15161−3827, IGR J16056−6110, IGR J19405−3016 and IGR J21272+4241, have statistical significance of their IBIS detection between 4.5σ and 4.9σ. While *INTEGRAL* sources detected with significance above 5σ have a probability of less than 1% of being spurious (see Bird et al. 2007; Krivonos et al. 2007), detections with lower significance might actually have a larger probability of being not real. Therefore, we caution the reader that, because of this, the hard X-ray detection of the above sources may be spurious and that the proposed optical identification may not correspond to an actual object emitting at high energies above 20 keV.

With the approach illustrated above, we could eventually select 38 unidentified, unclassified or poorly studied *INTEGRAL* sources that are associated to arcsec-sized soft X-ray or radio error boxes, plus one object possibly associated with a peculiar optical source in the IBIS error circle.

Figures 1–5 report the optical fields of the 39 sources of the selected sample. The corresponding optical counterparts are indicated with tick marks. The list of identified *INTEGRAL* sources is reported in Table 1 (which we thoroughly describe in the next section).

[1] http://www.iasfbo.inaf.it/IGR/main.html

[2] Available at http://archive.eso.org/dss/dss

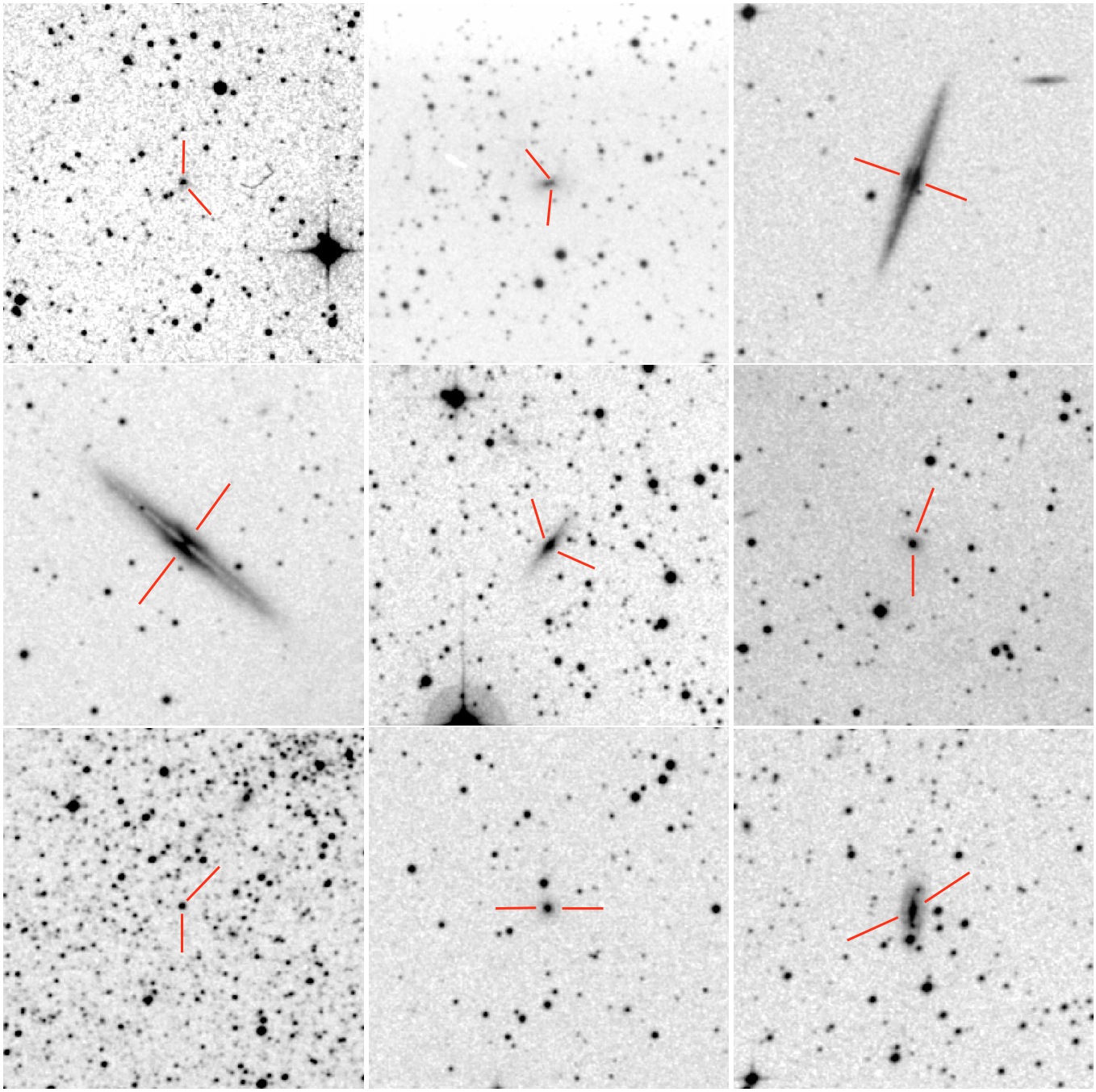

Fig. 1. *From left to right* and *top to bottom*: optical images of the fields of IGR J00040+7020, IGR J00256+6821, IGR J01528−0326, IGR J02343+3229, IGR J02504+5443, IGR J03334+3718, IGR J06117−6625, IGR J06292+4858 and IGR J07437−5147. The optical counterparts of the *INTEGRAL* sources are indicated with tick marks. Field sizes are $5' \times 5'$ and are extracted from the DSS-II-Red survey. In all cases, North is up and East to the left.

We here put forward that, for the high-energy sources with more than one optical candidate, we spectroscopically observed all objects with magnitude $R \lesssim 20$ within the longer-wavelength arcsec-sized error circle. However, in the following we will report only on their firm or likely optical counterparts, recognized via their peculiar spectral features (basically, the presence of emission lines). All other candidates are discarded because their spectra do not show any peculiarity (in general they are recognized as Galactic stars) and will not be considered further.

In our final sample one can also find the *INTEGRAL* objects mentioned by Torres et al. (2004); Negueruela & Smith (2006) and Burenin et al. (2006a,b; see also Halpern 2006). These objects, although already identified by means of preliminary reports, still have fragmentary longer-wavelength information. Our observations are meant to confirm the identification and to improve classification and knowledge of these hard X-ray sources.

3. Optical spectroscopy

The data collected and presented in this work are the result of a multisite campaign that involved the following observatories and telescopes in the past 2 years:

– the 1.5 m at the Cerro Tololo Interamerican Observatory (CTIO), Chile;

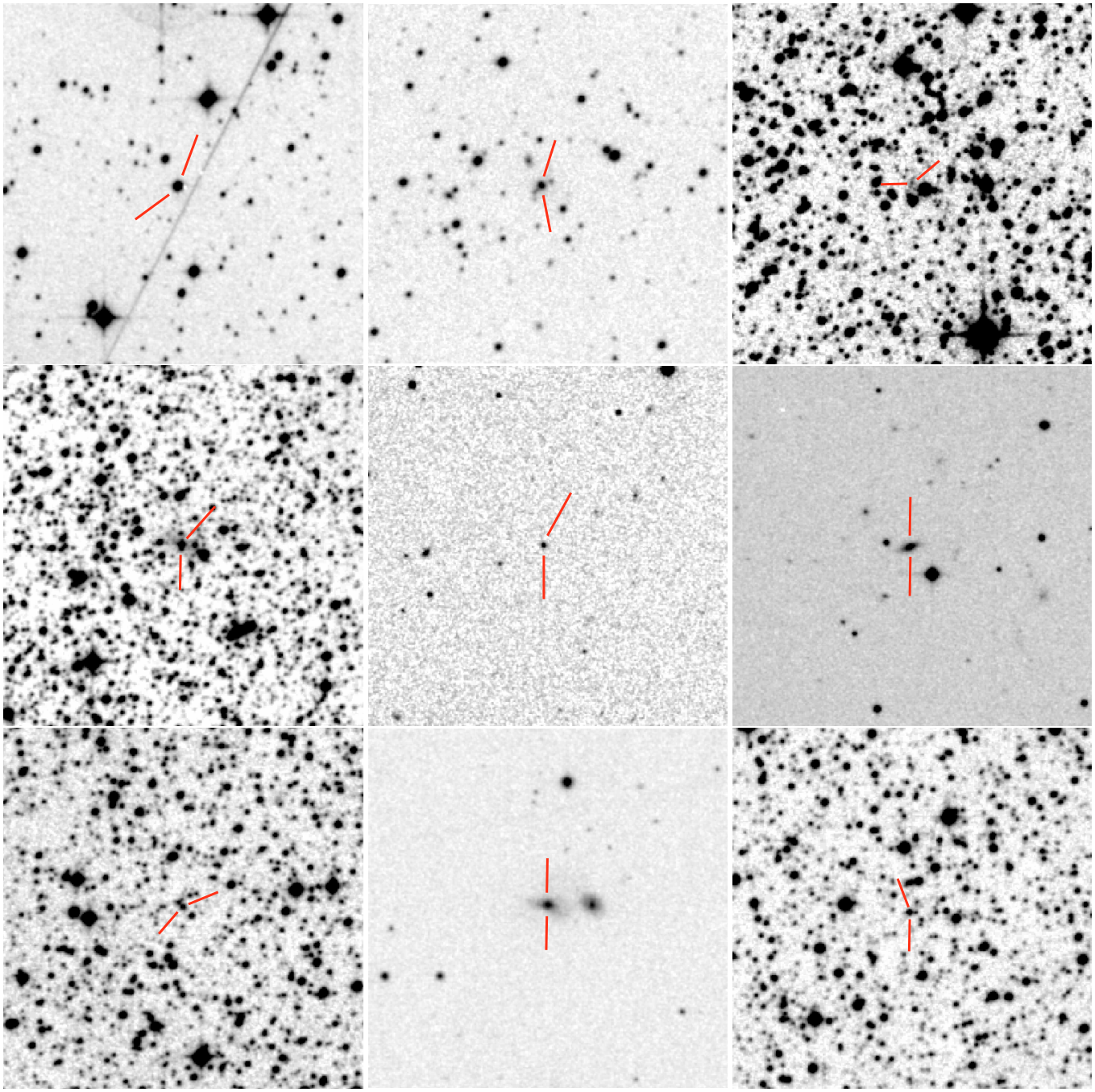

Fig. 2. As Fig. 1, but for the fields of IGR J08023−6954, IGR J09446−2636, IGR J09523−6231, IGR J11366−6002, IGR J12131+0700, IGR J13038+5348, IGR J13109−5552, IGR J13149+4422 and IGR J14298−6715.

– the 1.52 m "Cassini" telescope of the Astronomical Observatory of Bologna, in Loiano, Italy;
– the 1.8 m "Copernicus" telescope at the Astrophysical Observatory of Asiago, in Asiago, Italy;
– the 1.9 m "Radcliffe" telescope at the South African Astronomical Observatory (SAAO), in Sutherland, South Africa;
– the 2.15 m "Jorge Sahade" telescope at the Complejo Astronomico el Leoncito (CASLEO) in Argentina;
– the 3.5 m "New Technology Telescope" (NTT) and the 3.6 m telescope at the ESO-La Silla Observatory, Chile; and
– the 4.2 m "William Herschel Telescope" (WHT) at the Roque de Los Muchachos Observatory in La Palma, Spain.

The data taken by at these telescopes were reduced following standard procedures using IRAF[3]. Calibration frames (flat fields and lamps for wavelength calibration) were taken on the day preceeding or following the observing night. The wavelength calibration uncertainty was ~0.5 Å for all cases; this was checked using the positions of background night sky lines. Flux calibration was performed using catalogued spectrophotometric standards.

[3] IRAF is the Image Reduction and Analysis Facility made available to the astronomical community by the National Optical Astronomy Observatories, which are operated by AURA, Inc., under contract with the US National Science Foundation. It is available at http://iraf.noao.edu/

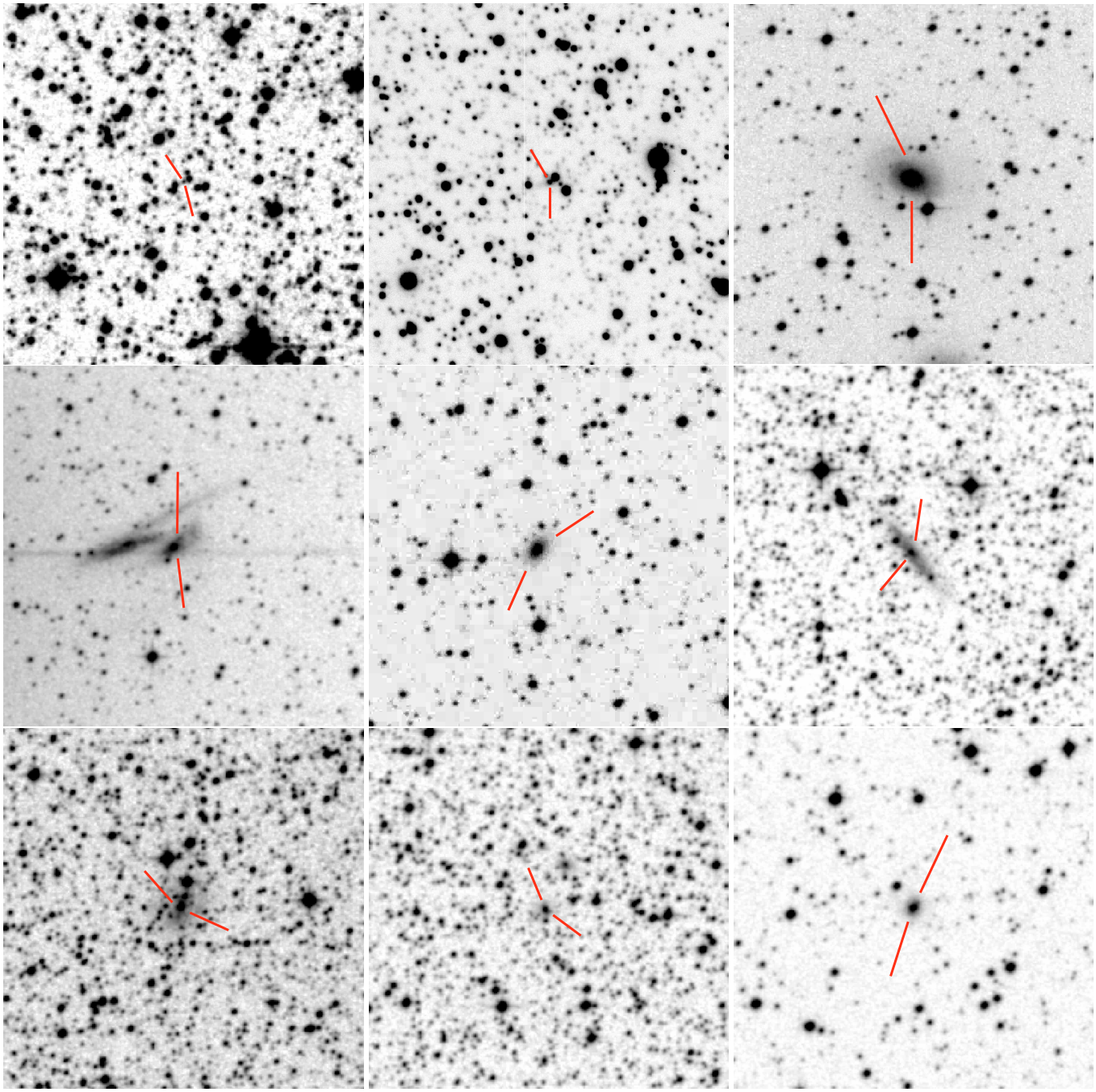

Fig. 3. As Fig. 1, but for the fields of IGR J14331−6112, IGR J14471−6414, IGR J14561−3738, IC 4518a, IGR J15161−3827, IGR J15539−6142, IGR J16024−6107, IGR J16056−6110 and IGR J16385−2057. The field of IGR J14471−6414 is $3' \times 3'$ in size and has been obtained at the ESO 3.6 m telescope using EFOSC2 and the *R* filter.

Moreover, further spectroscopic data were retrieved from two different astronomical archives. In particular, we retrieved 2 pipeline reduced spectra from the Sloan Digitized Sky Survey[4] (SDSS, Adelman-McCarthy et al. 2005) archive, and 4 from the Six-degree Field Galaxy Survey[5] (6dFGS) archive (Jones et al. 2004). As the 6dFGS archive provides spectra which are not calibrated in flux, we used the optical photometric information in Jones et al. (2005) and Doyle et al. (2005) to calibrate the 6dFGS data presented here.

We report in Table 1 the detalied log of observations. In particular we list in Col. 1 the name of the observed *INTEGRAL* sources. In Cols. 2 and 3 we report the object coordinates, extracted from the 2MASS catalogue (with an accuracy of $\leq 0\farcs1$, according to Skrutskie et al. 2006) or from the DSS-II-Red astrometry (which has an accuracy of $\sim 1''$). In Col. 4 we list the telescope and the instrument used for the observations. The characteristic of each spectrograph are given in Cols. 5 and 6. Column 7 provides the observation date and the UT time at mid-exposure, while Col. 8 reports the exposure times and the number of spectral pointings.

[4] http://www.sdss.org
[5] http://www.aao.gov.au/local/www/6df/

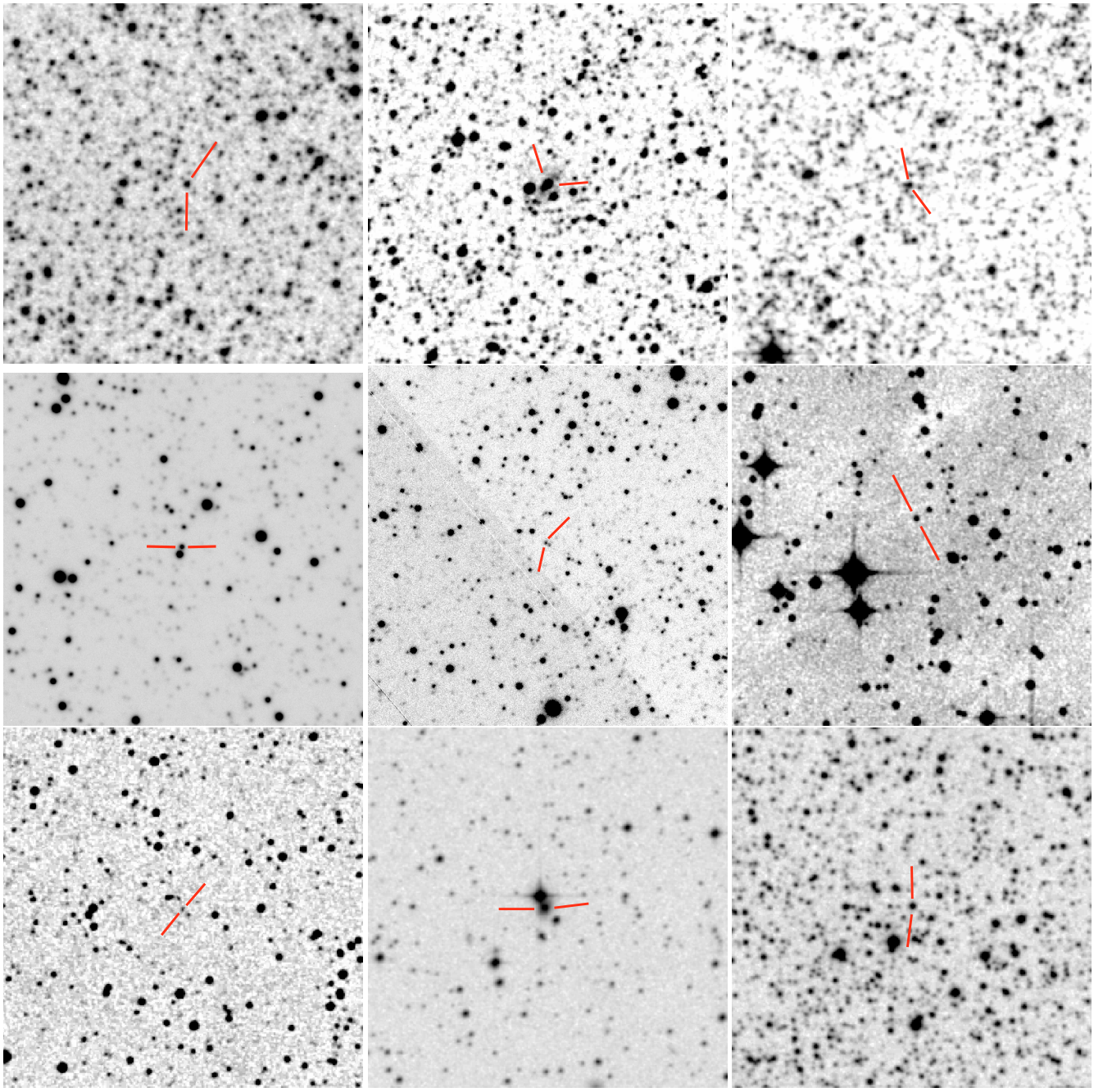

Fig. 4. As Fig. 1, but for the fields of IGR J16500−3307, 2E 1739.1−1210, 1RXS J174607.8−213333, SAX J1802.7−2017, IGR J18048−1455, SAX J1818.6−1703, IGR J18483−0311, IGR J19405−3016 and Swift J2000.6+3210. The fields of SAX J1802.7−2017 and IGR J18048−1455 are 3′ × 3′ in size and were obtained at the ESO 3.6 m telescope with EFOSC2 plus the *R* filter.

As a complement to the information on the putative counterparts of IGR J14331−6112, SAX J1802.7−2017 and IGR J18048−1455, we analyzed optical *R*-band frames acquired in parallel with the corresponding spectroscopic pointings on these sources. The field of SAX J1802.7−2017 was observed with NTT plus EMMI on 28 July 2007 (start time: 02:01 UT; duration: 10 s) under a seeing of 1.″5; the 2 × 2-rebinned CCDs of EMMI secured a plate scale of 0.″33/pix, and a useful field of 9.′9×9.′1. A 20-s image of the field of IGR J14331−6112 was obtained on 2007 June 22 (start time: 04:21 UT) with the 3.6 m ESO telescope plus EFOSC2 under a seeing of 1.″2; for the field of IGR J18048−1455, a 10-s image was acquired on 2007 June 23 (start time: 06:13 UT) with the same setup as above under a seeing of 1.″7. These two images, 2 × 2 binned, had a scale of 0.″31/pix and covered a field of 5.′2 × 5.′2.

The corresponding imaging frames were corrected for bias and flat-field in the usual fashion and calibrated using nearby USNO-A2.0[6] stars. Simple aperture photometry, within the MIDAS[7] package, was then used to measure the *R*-band magnitude of the putative optical counterparts of IGR J14331−6112, SAX J1802.7−2017 and IGR J18048−1455.

[6] Available at
http://archive.eso.org/skycat/servers/usnoa/
[7] http://www.eso.org/projects/esomidas

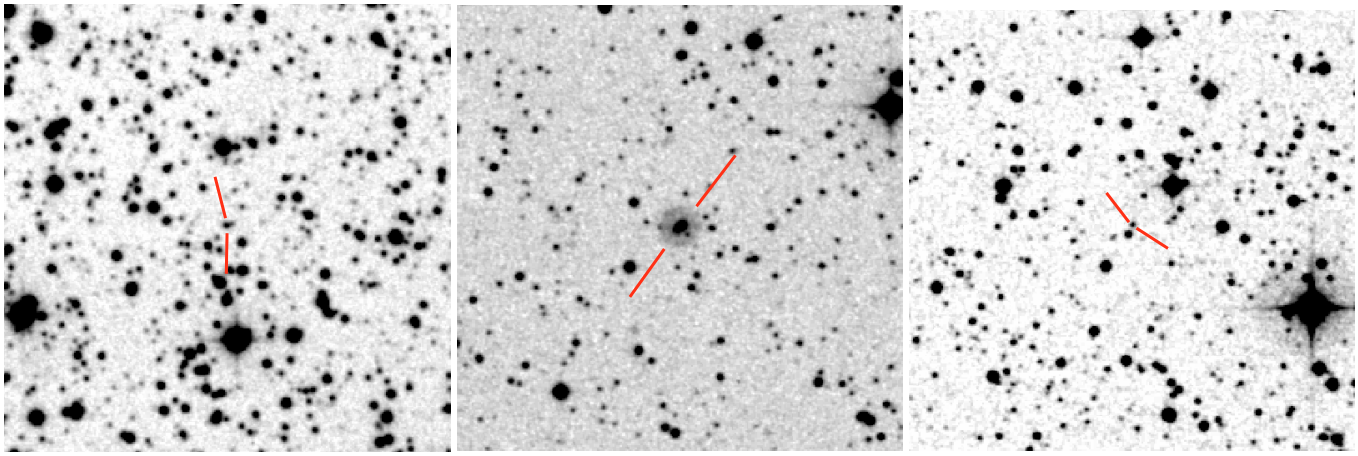

Fig. 5. As Fig. 1, but for the fields of IGR J21272+4241 (*left panel*), IGR J23308+7120 (*middle panel*) and IGR J23542+5842 (*right panel*).

4. Results

In this section we present the results of our spectroscopic campaign described in Sect. 3. The optical magnitudes quoted below, if not otherwise stated, are extracted from the USNO-A2.0 catalogue.

As already done in Papers I–V, we use the following identification and classification criteria for the optical spectra of the sources considered in this work.

For the determination of the distance of compact Galactic X-ray sources, in the case of CVs we assumed an absolute magnitude $M_V \sim 9$ and an intrinsic color index $(V-R)_0 \sim 0$ mag (Warner 1995), whereas for HMXBs, when applicable, we used the intrinsic stellar color indices and absolute magnitudes as reported in Lang (1992) and Wegner (1994). For low-mass X-ray binaries (LMXBs), we considered $(V-R)_0 \sim 0 \sim M_R$ (e.g., van Paradijs & McClintock 1995).

For the emission-line AGN classification, we used the criteria of Veilleux & Osterbrock (1987) and the line ratio diagnostics of Ho et al. (1993, 1997) and of Kauffmann et al. (2003); moreover, for the subclass assignation of Seyfert 1 nuclei, we used the H_β/[O III]λ5007 line flux ratio criterion as per Winkler (1992).

When possible in the cases of extragalactic objects, for the calculation of the intrinsic absorption in the host galaxy of a line-emitting AGN we first dereddened the H_α and H_β line fluxes by applying a correction for the Galactic absorption along the source line of sight. This was done following the prescription for the computation of the Galactic color excess $E(B-V)_{\rm Gal}$ given by Schlegel et al. (1998), and considering the Galactic extinction law by Cardelli et al. (1989). Then, we assumed an intrinsic H_α/H_β line ratio of 2.86 (Osterbrock 1989) and we computed the color excess $E(B-V)_{\rm AGN}$ local to the AGN host, using again Cardelli et al.'s (1989) extinction law, from the comparison between the intrinsic line ratio and the one corrected for the Galactic reddening.

The spectra of the galaxies shown here were not corrected for starlight contamination (see, e.g., Ho et al. 1993, 1997) given the limited S/N and the spectral resolution. We do not consider this to affect any of our conclusions.

In the following we assume a cosmology with $H_0 = 65$ km s^{-1} Mpc^{-1}, $\Omega_\Lambda = 0.7$ and $\Omega_{\rm m} = 0.3$; the luminosity distances of the extragalactic objects reported in this paper are computed with these parameters using the Cosmology Calculator of Wright (2006). Moreover, when not explicitly stated otherwise, for our X-ray flux estimates we will assume a Crab-like spectrum except for the *XMM-Newton* Slew Survey sources, for which we considered the 0.2–12 keV flux reported by Saxton et al. (2008). We also remark that the results presented here supersede the preliminary ones reported in Masetti et al. (2006e,f, 2007a,b).

The next subsections report the object identifications divided into three broad classes (CVs, X-ray binaries and AGNs) ordered according to their increasing distance from Earth; two more sources (IGR 06292+4858 and IGR J08023−6954) are discussed in a separate Subsection due to the peculiarities about their identification, as stressed in Sect. 2.

4.1. CVs

One object of our sample, IGR J16500−3307, was identified as a dwarf nova CV through the appearance of its optical spectrum (Fig. 6, left panel). It shows Balmer emissions up to at least H_δ, as well as several He I and He II lines in emission. All of the detected lines are consistent with being at $z = 0$, indicating that this object belongs to our Galaxy. In addition, source 1RXS J174607.8−213333 was identified as a symbiotic star, given that its optical spectral continuum shows the typical characteristics of a red giant star with superimposed Balmer emissions at $z = 0$ (Fig. 6, right panel).

The main spectral characteristics for the two objects, and the parameters which can be inferred from their optical and X-ray data, are listed in Table 2. The fact that, in the spectrum of IGR J16500−3307, the He IIλ4686/H_β equivalent width (EW) ratio is $\gtrsim$0.5 and the EWs of He II and H_β are around 10 Å indicates that this source is a magnetic CV belonging to the intermediate polar (IP) subclass (see Warner 1995 and references therein). Its optical spectrum, moreover, closely resembles those of other CVs detected with *INTEGRAL* (Papers IV and V), and which were classified as IPs. For this source, we determine the reddening along its line of sight as $A_V = 0.53$ mag, inferred by comparing the observed H_α/H_β flux ratio with an assumed intrinsic one of 2.86 (Osterbrock 1989) and then applying the Cardelli et al.'s (1989) Galactic extinction law.

Using the Bruzual-Persson-Gunn-Stryker[8] (Gunn & Stryker 1983) and Jacoby-Hunter-Christian[9] (Jacoby et al. 1984) spectroscopy atlases, we constrained the spectral type of the optical counterpart of 1RXS J174607.8−213333 to be between M2 III and M4 III. From this information, assuming the colors and absolute V magnitude of a M3 III star (Ducati et al. 2001;

[8] Available at: ftp://ftp.stsci.edu/cdbs/cdbs1/grid/bpgs/
[9] Available at: ftp://ftp.stsci.edu/cdbs/cdbs1/grid/jacobi/

Table 1. Log of the spectroscopic observations presented in this paper (see text for details). If not otherwise indicated, source coordinates are extracted from the 2MASS catalogue and have an accuracy better than 0.″1.

Object	RA (J2000)	Dec (J2000)	Telescope+instrument	λ range (Å)	Disp. (Å/pix)	UT Date and Time at mid-exposure	Exposure time (s)
IGR J00040+7020	00:04:01.92	+70:19:18.5	Copernicus+AFOSC	4000–8000	4.2	27 Nov. 2006, 20:23	3 × 1800
IGR J00256+6821	00:25:32.5†	+68:21:44†	Cassini+BFOSC	3500–8000	4.0	18 Nov. 2006, 21:42	3 × 1800
IGR J01528−0326	01:52:49.00	−03:26:48.5	AAT+6dF	3900–7600	1.6	02 Dec. 2002, 11:07	1200+600
IGR J02343+3229	02:34:20.10	+32:30:20.0	Cassini+BFOSC	3500–8000	4.0	03 Oct. 2006, 23:19	3 × 1800
IGR J02504+5443	02:50:42.59	+54:42:17.7	Copernicus+AFOSC	4000–8000	4.2	14 Nov. 2006, 01:25	2 × 2400
IGR J03334+3718	03:33:18.79	+37:18:11.1	Cassini+BFOSC	3500–8000	4.0	02 Oct. 2006, 02:33	2 × 1800
IGR J06117−6625	06:11:48.34	−66:24:33.7	CTIO 1.5m+RC Spc.	3300–10500	5.7	19 Feb. 2007, 04:45	3 × 1800
IGR J06292+4858*	06:29:13.57	+49:01:24.9	Cassini+BFOSC	3500–8000	4.0	13 Dec. 2006, 23:52	2 × 1800
IGR J07437−5137*	07:43:31.71	−51:40:56.7	CTIO 1.5m+RC Spc.	3300–10500	5.7	20 Feb. 2007, 02:55	2 × 1800
IGR J08023−6954*	08:02:41.64	−69:53:37.7	CTIO 1.5m+RC Spc.	3300–10500	5.7	20 Feb. 2007, 01:57	2 × 900
IGR J09446−2636	09:44:37.02	−26:33:55.4	AAT+6dF	3900–7600	1.6	17 Mar. 2004, 12:00	1200+600
IGR J09523−6231	09:52:20.7†	−62:32:37†	3.6m+EFOSC	3685-9315	2.8	24 Jun. 2007, 00:27	2 × 1800
IGR J11366−6002	11:36:42.04	−60:03:06.6	NTT+EMMI	3300–9050	2.8	29 Jul. 2007, 23:15	2 × 300
IGR J12131+0700	12:12:49.81	+06:59:45.1	SDSS+CCD Spc.	3800–9200	1.0	16 Jan. 2005, 12:32	4000
IGR J13038+5348	13:03:59.43	+53:47:30.1	Cassini+BFOSC	3500–8000	4.0	13 Jan. 2007, 04:47	2 × 1200
IGR J13109−5552	13:10:43.35	−55:52:11.4	3.6m+EFOSC	3685–9315	2.8	21 Jun. 2007, 03:44	2 × 600
IGR J13149+4422	13:15:17.25	+44:24:25.9	SDSS+CCD Spc.	3800–9200	1.0	25 Mar. 2004, 09:11	1920
IGR J14298−6715	14:29:59.81	−67:14:44.8	3.6m+EFOSC	3685–9315	2.8	23 Jun. 2007, 02:26	2 × 360
IGR J14331−6112	14:33:08.33	−61:15:39.7	3.6m+EFOSC	3685–9315	2.8	22 Jun. 2007, 04:41	2 × 900
IGR J14471−6414	14:46:28.26	−64:16:24.3	3.6m+EFOSC	3685–9315	2.8	22 Jun. 2007, 05:34	2 × 1200
IGR J14561−3738*	14:56:08.43	−37:38:52.4	Jorge Sahade+REOSC	3890–7360	3.4	11 Mar. 2007, 05:37	2 × 1200
IC 4518a	14:57:41.16	−43:07:55.2	CTIO 1.5m+RC Spc.	3300–10500	5.7	19 Feb. 2007, 08:44	2 × 1200
IGR J15161−3827	15:15:59.70	−38:25:46.8	AAT+6dF	3900–7600	1.6	11 Mar. 2003, 16:30	1200+600
IGR J15539−6142	15:53:35.28	−61:40:58.4	Jorge Sahade+REOSC	3890–7360	3.4	11 Mar. 2007, 07:46	2 × 1200
IGR J16024−6107	16:01:48.23	−61:08:54.7	Radcliffe+Grating Spc.	3850–7200	2.3	26 Apr. 2007, 01:15	2 × 1200
IGR J16056−6110	16:05:51.17	−61:11:44.0	Jorge Sahade+REOSC	3890–7360	3.4	12 Mar. 2007, 05:16	2 × 1800
IGR J16385−2057	16:38:30.91	−20:55:24.6	AAT+6dF	3900–7600	1.6	08 Jun. 2003, 14:05	1200+600
IGR J16500−3307	16:49:55.64	−33:07:02.0	Jorge Sahade+REOSC	3890–7360	3.4	12 Mar. 2007, 08:02	2 × 1800
2E 1739.1−1210	17:41:55.25	−12:11:56.6	3.6m+EFOSC	3685–9315	2.8	25 Jun. 2007, 01:13	300
1RXS J174607.8−213333	17:46:03.16	−21:33:27.1	CTIO 1.5m+RC Spc.	3300–10500	5.7	16 Jun. 2007, 05:32	2 × 1200
SAX J1802.7−2017	18:02:41.94	−20:17:17.2	NTT+EMMI	3300–9050	2.8	28 Jul. 2007, 01:27	2 × 600
IGR J18048−1455	18:04:38.92	−14:56:47.4	3.6m+EFOSC	3685–9315	2.8	23 Jun. 2007, 06:35	2 × 1200
SAX J1818.6−1703	18:18:37.90	−17:02:47.9	3.6m+EFOSC	3685–9315	2.8	23 Jun. 2007, 08:37	2 × 1200
IGR J18483−0311	18:48:17.20	−03:10:16.8	3.6m+EFOSC	3685–9315	2.8	22 Jun. 2007, 06:21	2 × 1200
IGR J19405−3016	19:40:15.07	−30:15:52.2	Radcliffe+Grating Spc.	3850–7200	2.3	30 Apr. 2007, 04:10	2 × 900
Swift J2000.6+3210	20:00:21.85	+32:11:23.2	Cassini+BFOSC	3500–8000	4.0	13 Jul. 2006, 23:19	2 × 1800
IGR J21272+4241	21:27:18.51	+42:39:11.2	WHT+ISIS	5050–10300	1.8	01 Sep. 2007, 02:40	2 × 400
IGR J23308+7120	23:30:37.68	+71:22:46.6	Cassini+BFOSC	3500–8000	4.0	25 Jul. 2007, 01:45	2 × 1800
IGR J23524+5842	23:52:22.11	+58:45:30.7	WHT+ISIS	5050–10300	1.8	01 Sep. 2007, 03:10	2 × 900

* Source with tentative optical identification; † coordinates extracted from the DSS-II-Red frames, having an accuracy of ∼1″.

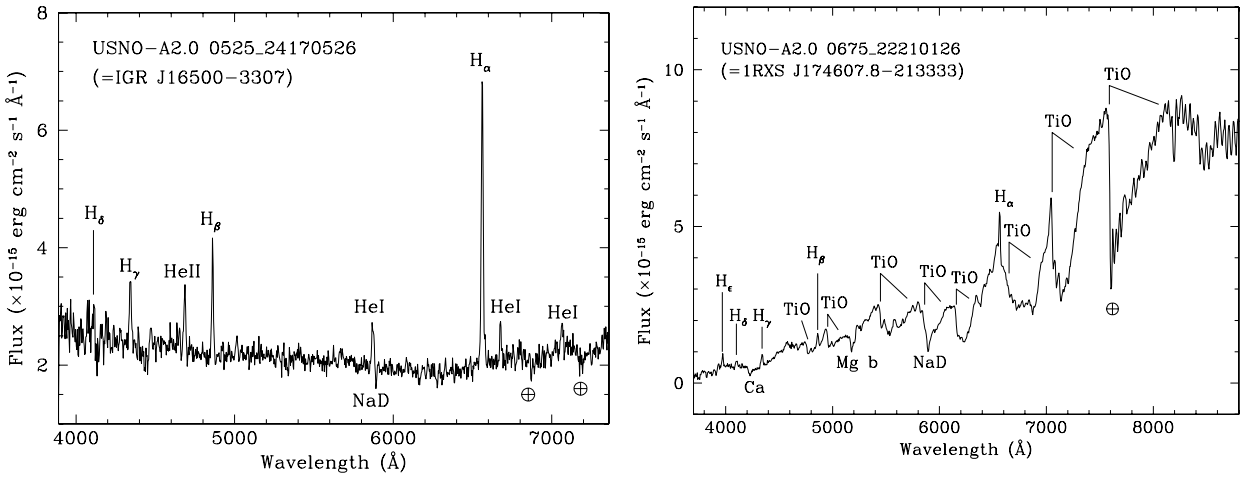

Fig. 6. Spectra (not corrected for the intervening Galactic absorption) of the optical counterparts of the CVs belonging to the *INTEGRAL* sources sample presented in this paper. For each spectrum the main spectral features are labeled. The symbol ⊕ indicates atmospheric telluric absorption bands.

Table 2. Synoptic table containing the main results concerning the 2 CVs (see Fig. 6) identified in the present sample of *INTEGRAL* sources.

Object	H_α		H_β		He II λ4686		R	d	L_X
	EW	Flux	*EW*	Flux	*EW*	Flux	mag	(pc)	
IGR J16500−3307	35.2 ± 0.2	7.1 ± 0.4	9.9 ± 1.0	2.1 ± 0.2	7.1 ± 0.7	1.59 ± 0.16	16.0	∼210	0.022 (0.1–2.4) 1.0 (20–100)
1RXS J174607.8−213333	5.2 ± 0.5	2.1 ± 0.2	7.1 ± 0.7	0.84 ± 0.08	<1	<0.1	14.7	<21 800	<10 500 (18–60)

Note: *EW*s are expressed in Å, line fluxes are in units of 10^{-14} erg cm^{-2} s^{-1}, whereas X-ray luminosities are in units of 10^{32} erg s^{-1} and the reference band (between brackets) is expressed in keV.

Table 3. Synoptic table containing the main results concerning the 5 HMXBs (see Fig. 7) identified or observed in the present sample of *INTEGRAL* sources.

Object	H_α		Optical	A_V	d	Spectral	L_X
	EW	Flux	mag.	(mag)	(kpc)	type	
IGR J14331−6112	4.6 ± 0.5	0.027 ± 0.003	18.1 (*R*)	≈6.5	≈10	early B III or mid B V	0.054 (2–10) 0.15 (20–100)
SAX J1802.7−2017	4.2 ± 0.6	0.074 ± 0.011	16.9 (*R*)	∼8.3	≈10	early B III	1.1[a] (2–10) 0.75 (20–100)
SAX J1818.6−1703	3.2 ± 0.6[b]	0.0124 ± 0.0013[b]	17.4 (*R*)	∼14	∼2.5	OB supergiant	0.0056[c] (0.5–10) 0.018[c] (20–100)
IGR J18483−0311	8.5 ± 2.6	0.0089 ± 0.0027	19.3[d] (*R*)	≈13[d]	∼3.5[d]	OB giant	0.0063[c] (1–7) 0.088[c] (20–100)
Swift J2000.6+3210	10.2 ± 0.5	1.88 ± 0.09	16.1 (*R*)	∼4.0	≈8	early B V or mid B III	≈0.038 (0.2–12) ≈0.25 (20–100)

Note: *EW*s are expressed in Å, line fluxes are in units of 10^{-14} erg cm^{-2} s^{-1}, whereas X-ray luminosities are in units of 10^{36} erg s^{-1} and the reference band (between brackets) is expressed in keV. [a] luminosity estimate from Hill et al. (2005); [b] sum of two components; [c] low-state luminosity values; [d] from Sguera et al. (2007).

Lang 1992), we obtain a distance of ∼22 kpc for the source, which would place it on the other side of the Galaxy, beyond the Bulge. This suggests that some amount of absorption should be present along the line of sight and that this number should rather be used as an (admittedly loose) upper limit for the distance to this object.

The X-ray luminosities for the two objects were then computed using the fluxes reported in Bird et al. (2007) and Revnivtsev et al. (2004a).

We conclude this section by mentioning that, although 1RXS J174607.8−213333 is present in the survey of Revnivtsev et al. (2004a), it does not appear in the deeper IBIS surveys of Bird et al. (2007) and of Krivonos et al. (2007). This may suggest either some variability of this X-ray source, or that the *INTEGRAL* detection reported by Revnivtsev et al. (2004a) is spurious. Nevertheless, the *Swift*/XRT observation indicates that X-ray activity up to 10 keV is in any case produced by the symbiotic system identified here.

4.2. X-ray binaries

4.2.1. HMXBs

We classify 5 of the *INTEGRAL* sources of our sample as HMXBs by their overall spectral appearance (see Fig. 7), which is typical of this class of objects (see e.g. Papers III and V), with narrow H_α emission at a wavelength consistent with that of the laboratory restframe, superimposed on an intrinsically blue continuum with Balmer absorptions. Practically in all cases, however, the stellar continuum appears strongly reddened and sometimes almost undetected bluewards of 5000 Å, implying the presence of substantial interstellar dust along the line of sight. This also is quite typical of HMXBs detected with *INTEGRAL* (e.g., Paper V) and indicates that these objects are relatively far from Earth.

Table 3 collects the relevant optical spectral information on these 5 sources, along with their main parameters inferred from the available optical and X-ray data. Luminosities for these objects were calculated using the X-ray fluxes of Bird et al. (2007), Saxton et al. (2008), in 't Zand et al. (2006), Sguera et al. (2007) and Landi et al. (2007b).

Below we report on results concerning the optical counterparts of these 5 hard X-ray sources.

The optical spectrum of the counterpart of SAX J1818.6−1703 seems to show a faint, double-peaked H_α emission, with the blue peak twice as faint with respect to the red one. The two peaks appear to be separated by $\Delta\lambda \sim 8.5$ Å.

The *EW* of the H_α emission line detected in the optical spectrum of IGR J18483−0311 appears too large for a supergiant secondary star (see Leitherer 1988). Thus, together with the use of the results reported in Sguera et al. (2007), we infer that this HMXB hosts a secondary star of intermediate luminosity class. This allows us to determine distance and X-ray luminosities for this source as reported in Table 3.

Our *R*-band photometry of the counterparts of IGR J14331−6112 and SAX J1802.7−2017 yields magnitudes $R = 18.1 \pm 0.1$ and $R = 16.9 \pm 0.1$, respectively. Unfortunately, due to a general lack of reliable multifilter optical photometry for the counterparts of the HMXBs considered here (in particular for

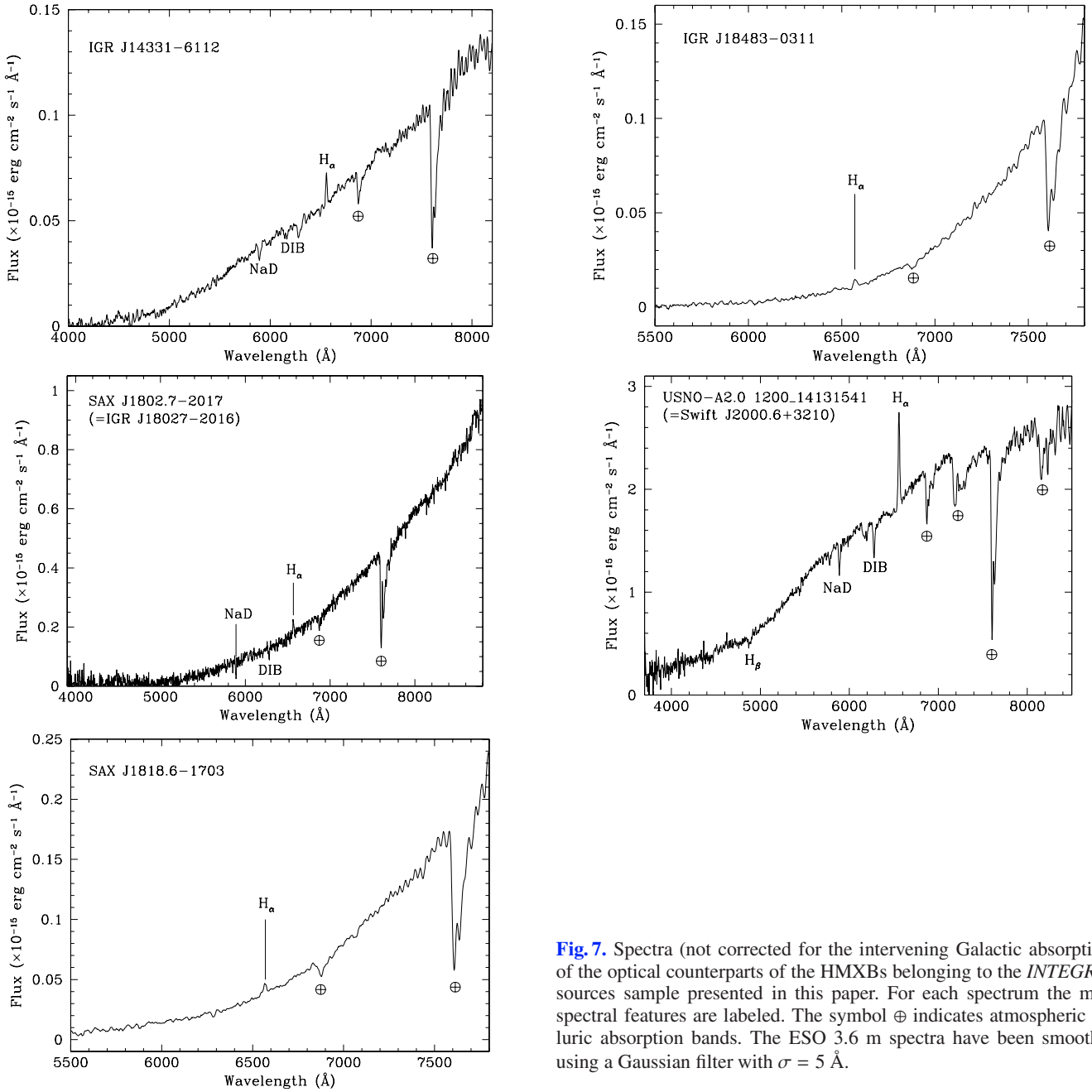

Fig. 7. Spectra (not corrected for the intervening Galactic absorption) of the optical counterparts of the HMXBs belonging to the *INTEGRAL* sources sample presented in this paper. For each spectrum the main spectral features are labeled. The symbol ⊕ indicates atmospheric telluric absorption bands. The ESO 3.6 m spectra have been smoothed using a Gaussian filter with σ = 5 Å.

IGR J14331−6112 and Swift J2000.6+3210), no precise information concerning distance, spectral type and X-ray luminosity can be determined.

For SAX J1802.7−2017 this problem can be circumvented by using the information in Hill et al. (2005). Indeed, using the mass and radius estimates of these authors and comparing them with the tabulated values for early-type stars in Lang (1992), we conclude that the optical companion in this wind-fed X-ray system is likely an early B giant. We note this is at odds with the companion star classification of Hill et al. (2005), who suggested an early-type supergiant star on the basis of the position of the X-ray source in the Corbet's (1986) $P_{\rm orb}$−$P_{\rm spin}$ diagram. However, were it a HMXB with an OB supergiant, it would be placed at a distance of ∼18 kpc, on the other side of the Galaxy. This would make it hardly detectable at optical wavelengths because of strong reddening due to the presence of large amounts of intervening Galactic dust.

Concerning SAX J1818.6−1703, we derived the distance using the magnitudes reported in Negueruela & Smith (2006) and assuming that the counterpart is an OB supergiant as suggested by Negueruela et al. (2007).

In the cases of IGR J14331−6112 and Swift J2000.6+3210, however, by considering the absolute magnitudes of early-type stars and by applying the method described in Paper III for the classification of source 2RXP J130159.6−635806, we obtained the constraints for distance, reddening, spectral type and X-ray luminosity shown in Table 3.

Sguera et al. (2007) found for IGR J18483−0311, from the comparison between the line-of sight absorptions derived from the optical reddening A_V and from the hydrogen column density $N_{\rm H}$ inferred from the source X-ray spectra, that the latter one appears to be larger. We can make a similar comparison considering the two more HMXBs reported in this Section for which an $N_{\rm H}$ measurement is available, that is, SAX J1802.7−2017

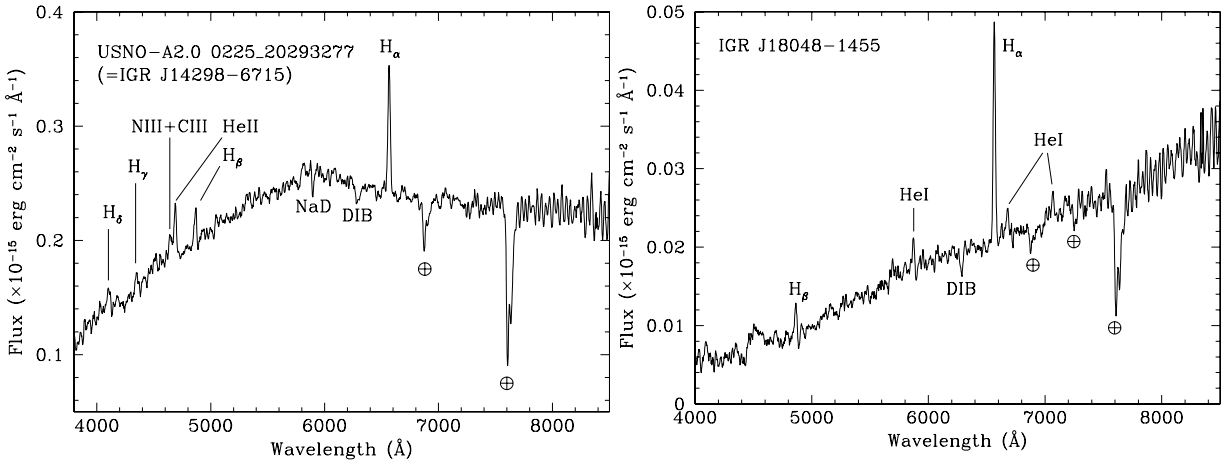

Fig. 8. Spectra (not corrected for the intervening Galactic absorption) of the optical counterparts of the LMXBs belonging to the *INTEGRAL* sources sample presented in this paper. For each spectrum the main spectral features are labeled. The symbol ⊕ indicates atmospheric telluric absorption bands. Both spectra have been smoothed using a Gaussian filter with σ = 5 Å.

Table 4. Synoptic table containing the main results concerning the 2 LMXBs (see Fig. 8) identified in the present sample of *INTEGRAL* sources.

Object	H_α		H_β		He II λ4686		R	d	L_X
	EW	Flux	*EW*	Flux	*EW*	Flux	mag	(kpc)	
IGR J14298−6715	12.0 ± 0.6	28.9 ± 1.4	4.1 ± 0.4	8.1 ± 0.8	8.0 ± 0.8	14.6 ± 1.5	16.4 (*R*)	∼10	0.31 (2–10) 1.5 (20–100)
IGR J18048−1455	29.4 ± 1.5	6.2 ± 0.3	9.6 ± 2.9	0.85 ± 0.26	<14	<1.0	18.7 (*R*)	∼7	0.72 (20–100)

Note: *EW*s are expressed in Å, line fluxes are in units of 10^{-16} erg cm^{-2} s^{-1}, whereas X-ray luminosities are in units of 10^{35} erg s^{-1} and the reference band (between brackets) is expressed in keV.

(Walter et al. 2006) and SAX J1818.6−7103 (in 't Zand et al. 2006). Using the empirical foumula of Predehl & Schmitt (1995), we find that in the two cases the X-ray absorption is two to five times larger than that determined in the optical. This is often observed in absorbed HMXBs detected with *INTEGRAL* (e.g., Chaty 2007) and suggests the presence of additional absorbing material in the vicinity of the X-ray source, likely due to the accretion stream flowing onto the compact object in these X-ray systems.

We conclude this Section by noting that none of these sources is associated with a radio source. This means that none of them is likely a jet-emitting HMXB (i.e., a microquasar).

4.2.2. LMXBs

Two hard X-ray sources of our sample, IGR J14298−6715 and IGR J18048−1455, show Balmer and helium emission lines at z = 0 superimposed on a reddened continuum (see Fig. 8). This again tells us that these two objects are Galactic X-ray systems. Furthermore, we measure a magnitude R = 18.7 ± 0.1 for the counterpart of IGR J18048−1455.

The shape of the optical continuum of these two sources does not show features of a red giant star (as in the case of 1RXS J174607.8−213333), and thus suggests that these objects are not intrinsically red but actually substantially absorbed; therefore, they are likely quite far from Earth. Because of this, we can exclude that they are CVs.

We can also rule out an HMXB nature for them because their optical and 2MASS near-infrared (NIR) magnitudes do not fit any star of early spectral type, not even if absorption along the line of sight is taken into account (see below). We thus suggest that these two hard X-ray sources are LMXBs.

Confirmation of the presence of reddening along the line of sight of these sources comes from the observed H_α/H_β line ratio for the two cases, which implies A_V = 0.56 mag and 2.96 mag for IGR J14298−6715 and IGR J18048−1455, respectively. It should be noted, however, that if we correct the magnitudes of the counterparts with these figures, we obtain distances which are exceedingly large (>15 kpc). This suggests that the assumption we made on the intrinsic H_α/H_β line ratio in these sources is not correct; we thus consider it safer to use the Galactic color excess measure along the lines of sight, that is, $E(B-V)_{\rm Gal}$ = 0.516 mag for IGR J14298−6715 and $E(B-V)_{\rm Gal}$ = 1.787 mag for IGR J18048−1455. Assuming these estimates, optical and 2MASS magnitudes become compatible with those of persistent LMXBs, and we obtain the distances and X-ray luminosities reported in Table 4. In this table, the X-ray luminosities were computed using the fluxes reported in Bird et al. (2007) and in Landi et al. (2007b).

We thus here revise the classification of IGR J18048−1455 as a HMXB given by Burenin et al. (2006a); we also note that the authors report a value for the H_α *EW* of this source which is half of the one we measure in our optical spectrum. This hints to long-term variability of H_α emission in this object, which is not unusual in LMXBs.

4.3. AGNs

Globally, 28 objects of our sample show optical spectra which are dominated by redshifted broad and/or narrow emission lines typical of AGNs. We classify slightly more than half of this subsample (15 objects) as genuine or likely Seyfert 2 galaxies; three of them appear to be borderline objects between Seyfert 2 s and LINERs. The remaining 13 sources have been identified as Seyfert 1 galaxies: in detail, 4 are classified as Seyfert 1.2, 4 as

Table 5. Synoptic table containing the main results concerning the 13 broad emission line AGNs (see Figs. 9 and 10) identified or observed in the present sample of *INTEGRAL* sources.

Object	F_{H_α}	F_{H_β}	$F_{[OIII]}$	Class	z	D_L (Mpc)	$E(B-V)_{Gal}$	L_X
IGR J03334+3718	*	3.9 ± 0.2	3.3 ± 0.2	Sy1.5	0.055	264.3	0.535	0.33 (0.1–2.4)
	*	[19 ± 1]	[17 ± 1]					16.4 (17–60)
IGR J06117−6625	*	3.1 ± 0.2	1.82 ± 0.09	Sy1.5	0.230	1234.8	0.063	20.0 (0.1–2.4)
	*	[3.7 ± 0.2]	[2.12 ± 0.11]					529.5 (20–100)
IGR J09446−2636	*	3.5 ± 0.3	2.31 ± 0.12	Sy1.5	0.1425	726.2	0.086	10.1 (0.1–2.4)
	*	[4.5 ± 0.5]	[2.82 ± 0.14]					246.1 (17–60)
IGR J09523−6231	*	0.019 ± 0.004	0.19 ± 0.01	Sy1.9	0.252	1369.4	0.304	42.4 (0.2–12)
	*	[0.040 ± 0.008]	[0.40 ± 0.02]					279.4 (20–100)
IGR J12131+0700	*	0.052 ± 0.005	1.53 ± 0.05	Sy1.5/1.8	0.2095	1111.7	0.017	2.2 (2–10)
	*	[0.064 ± 0.006]	[1.63 ± 0.05]					290.0 (20–100)
IGR J13038+5348	*	21 ± 1	4.4 ± 0.2	Sy1.2	0.030	141.5	0.020	0.079 (0.1–2.4)
	*	[22 ± 1]	[4.7 ± 0.2]					7.5 (17–60)
IGR J13109−5552	*	—	0.022 ± 0.009	Sy1	0.104	516.9	0.325	18.2 (0.2–12)
	*	—	[0.053 ± 0.011]					77.2 (20–100)
IGR J14471−6414	*	0.12 ± 0.02	0.030 ± 0.003	Sy1.2	0.053	254.3	0.814	3.7 (2–10)
	*	[1.6 ± 0.3]	[0.36 ± 0.04]					9.3 (20–100)
IGR J16056−6110	*	8.0 ± 0.8	5.76 ± 0.03	Sy1.5	0.052	249.3	0.259	0.52 (0.1–2.4)
	*	[16.7 ± 1.7]	[12.6 ± 0.6]					1.0 (2–10)
								11.9 (20–100)
IGR J16385−2057	*	9.0 ± 0.9	1.3 ± 0.1	NLSy1	0.0269	126.6	0.500	0.53 (0.1–2.4)
	*	[44 ± 4]	[22 ± 2]					3.1 (20–100)
2E 1739.1−1210	*	2.0 ± 0.5	0.53 ± 0.05	Sy1.2	0.037	175.5	0.573	0.59 (0.1–2.4)
	*	[16 ± 3]	[2.2 ± 0.2]					3.7 (0.4–4)
								10.1 (20–100)
IGR J19405−3016	*	4.7 ± 0.3	1.47 ± 0.07	Sy1.2	0.052	249.3	0.103	2.6 (0.1–2.4)
	*	[6.1 ± 0.4]	[2.0 ± 0.1]					0.82 (2–10)
								13.5 (20–100)
IGR J21272+4241	0.14 ± 0.01	0.068 ± 0.014	0.229 ± 0.012	Sy1.8/1.9	0.316	1788.9	0.412	10.1 (2–10)
	[0.268 ± 0.013]	[0.18 ± 0.04]	[0.60 ± 0.04]					260.6 (20–40)
								<180.2 (40–100)

Note: emission line fluxes are reported both as observed and (between square brackets) corrected for the intervening Galactic absorption $E(B-V)_{Gal}$ along the object line of sight. Line fluxes are in units of 10^{-14} erg cm^{-2} s^{-1}, whereas X-ray luminosities are in units of 10^{43} erg s^{-1} and the reference band (between round brackets) is expressed in keV. Errors and limits are at 1σ and 3σ confidence levels, respectively. The typical error on the redshift measurement is ±0.001 but for the SDSS and 6dFGS spectra, for which an uncertainty of ±0.0003 can be assumed.
* Heavily blended with [N II] lines.

Seyfert 1.5, one as borderline Seyfert 1.5/1.8, 2 as Seyfert 1.8 or Seyfert 1.9 and one as narrow-line (NL) Seyfert 1; for the case of IGR J13109−5552 only a general Seyfert 1 classification can be given due to its anomalous optical spectral appearance (see Fig. 9, lower left panel).

The main observed and inferred parameters for each object are reported in Tables 5 and 6 for the broad emission line and narrow emission line AGNs, respectively. We assumed a null local absorption for Seyfert 1 AGNs. In these tables, X-ray luminosities were computed from the fluxes reported in Bird et al. (2007), in Krivonos et al. (2007), in Landi et al. (2007b–f), in the *Rossi-XTE* All-Sky Slew Survey of Revnivtsev et al. (2004b), in the *XMM-Newton* Slew Survey (Saxton et al. 2008), or using the *ROSAT*/PSPC (Voges et al. 1999) and *Einstein*/IPC (Harris et al. 1994) countrates.

For 15 out of 28 objects reported in this section, the redshift value was determined for the first time using the data presented here. We remark that the redshift of IGR J16056−6110 given in our preliminary analysis (Masetti et al. 2007a) was incorrect; here we give the correct value. The redshifts of the remaining 13 sources are consistent with those reported in the literature except for galaxy LEDA 21656 (the putative optical counterpart of IGR J07347−5137), for which we measure $z = 0.025$ instead of $z = 0.0086$ as reported in the Hyperleda catalogue (Prugniel 2005).

For two of the hard X-ray objects in the sample (IGR J06117−6625 and IGR J12131+0700) we note that no entry with these names is found in any catalogue of *INTEGRAL* sources. This is because the identifications for these two objects, given in Bird et al. (2007) and based on positional grounds

Table 6. Synoptic table containing the main results concerning the 15 narrow emission line AGNs (see Figs. 11 and 12) identified or observed in the present sample of *INTEGRAL* sources.

Object	F_{H_α}	F_{H_β}	$F_{[OIII]}$	Class	z	D_L	$E(B-V)$		L_X
						(Mpc)	Gal.	AGN	
IGR J00040+7020	0.58 ± 0.06 [3.2 ± 0.3]	0.088 ± 0.006 [1.12 ± 0.16]	1.20 ± 0.06 [13.2 ± 0.7]	Sy2	0.096	474.6	0.843	0	11.4 (2–10) 39.1 (20–100)
IGR J00256+6821	0.23 ± 0.02 [2.5 ± 0.3]	<0.017 [<0.47]	0.31 ± 0.03 [7.9 ± 0.8]	Sy2	0.012	55.9	1.027	>0.63	0.019 (2–10) 0.53 (20–100)
IGR J01528−0326	7.8 ± 0.4 [8.2 ± 0.4]	in abs. ″	2.8 ± 0.8 [3.0 ± 0.8]	likely Sy2	0.0167	79.3	0.029	—	0.30 (2–10) 2.1 (20–100)
IGR J02343+3229	0.10 ± 0.01 [0.125 ± 0.012]	in abs. ″	0.32 ± 0.05 [0.42 ± 0.06]	Sy2/LINER	0.015	74.7	0.099	—	2.6 (17–60)
IGR J02504+5443	0.17 ± 0.02 [1.1 ± 0.1]	0.021 ± 0.006 [0.25 ± 0.07]	0.29 ± 0.05 [3.4 ± 0.5]	Sy2	0.015	70.0	0.774	0.45	0.28 (2–10) 1.9 (20–100)
IGR J07437−5137	1.12 ± 0.11 [2.2 ± 0.2]	in abs. ″	<0.1 [<0.16]	Sy2?	0.025	117.5	0.299	—	1.5 (20–40) <1.1 (40–100)
IGR J11366−6002	0.33 ± 0.03 [2.6 ± 0.3]	0.028 ± 0.008 [0.58 ± 0.17]	0.055 ± 0.008 [1.05 ± 0.16]	Sy2/LINER	0.014	65.3	0.940	0.47	0.23 (2–10) 0.66 (20–100)
IGR J13149+4422	4.49 ± 0.13 [4.57 ± 0.14]	0.90 ± 0.04 [0.95 ± 0.05]	2.04 ± 0.06 [2.17 ± 0.07]	Sy2/LINER	0.0353	167.2	0.019	0.52	9.7 (0.2–12) 7.2 (17–60)
IGR J14561−3738	3.8 ± 0.4 [4.5 ± 0.5]	in abs. ″	1.5 ± 0.3 [2.1 ± 0.4]	likely Sy2	0.024	112.7	0.084	—	0.62 (3–8) 0.88 (8–20) 2.1 (17–60)
IC 4518a	11 ± 1 [15.8 ± 1.6]	2.0 ± 0.1 [3.57 ± 0.18]	17.6 ± 0.5 [28.9 ± 0.9]	Sy2	0.016	75.9	0.157	0.44	1.5 (20–100)
IGR J15161−3827	13.2 ± 0.7 [16.3 ± 0.8]	2.69 ± 0.13 [3.9 ± 0.2]	6.14 ± 0.18 [8.5 ± 0.3]	Sy2	0.0365	173.0	0.099	0.38	0.86 (3–8) <1.3 (8–20) 5.4 (20–100)
IGR J15539−6142	5.7 ± 0.3 [12.3 ± 0.6]	<0.34 <0.98	1.4 ± 0.3 [4.5 ± 1.1]	Sy2	0.015	69.6	0.341	>1.50	1.2 (20–100)
IGR J16024−6107	3.04 ± 0.15 [6.6 ± 0.3]	0.57 ± 0.06 [2.0 ± 0.2]	1.01 ± 0.07 [2.9 ± 0.2]	Sy2	0.011	52.9	0.334	0.15	0.012 (0.1–2.4) 0.060 (2–10) 0.23 (20–40) <0.16 (40–100)
IGR J23308+7120	0.17 ± 0.03 [0.73 ± 0.15]	in abs. ″	0.27 ± 0.03 [2.0 ± 0.2]	likely Sy2	0.037	175.5	0.663	—	0.52 (2–10) 2.5 (20–40) <2.1 (40–100)
IGR J23524+5842	— —	<0.01 <0.3	0.06 ± 0.01 [1.9 ± 0.3]	likely Sy2	0.164	849.9	1.290	—	110.8 (20–100)

Note: emission line fluxes are reported both as observed and (between square brackets) corrected for the intervening Galactic absorption $E(B-V)_{Gal}$ along the object line of sight. Line fluxes are in units of 10^{-14} erg cm^{-2} s^{-1}, whereas X-ray luminosities are in units of 10^{43} erg s^{-1} and the reference band (between round brackets) is expressed in keV. Errors and limits are at 1σ and 3σ confidence levels, respectively. The typical error on the redshift measurement is ±0.001 but for the SDSS and 6dFGS spectra, for which an uncertainty of ±0.0003 can be assumed.

only, were not correct as these sources were labeled there as PKS 0611−663 and NGC 4180, respectively. As a matter of facts, however, the *ROSAT* and *Swift*/XRT positions of these two sources, respectively, indicate that actually the X-ray emitting objects within the corresponding *INTEGRAL* error boxes are not those initially reported in the 3rd IBIS Survey, but rather the ones presented here (see also the preliminary reports of Masetti et al. 2007a; and Landi et al. 2007e). Therefore, here we changed their names using the typical notation for the newly-identified *INTEGRAL* sources.

Moreover, we drop the statement made in Masetti et al. (2007a) concerning the possible Seyfert 2 nature of NGC 4180, given that no detectable X-ray emission is seen from the nucleus of this galaxy in the corresponding XRT pointing. There may be the possibility (as mentioned in Landi et al. 2007e) that the nucleus of NGC 4180 is extremely absorbed, being thus the actual responsible of the high-energy emission detected with *INTEGRAL* but on the contrary very faint below 10 keV; however, the presence of an X-ray emitting broad emission line AGN in the same IBIS error box makes this eventuality rather unlikely.

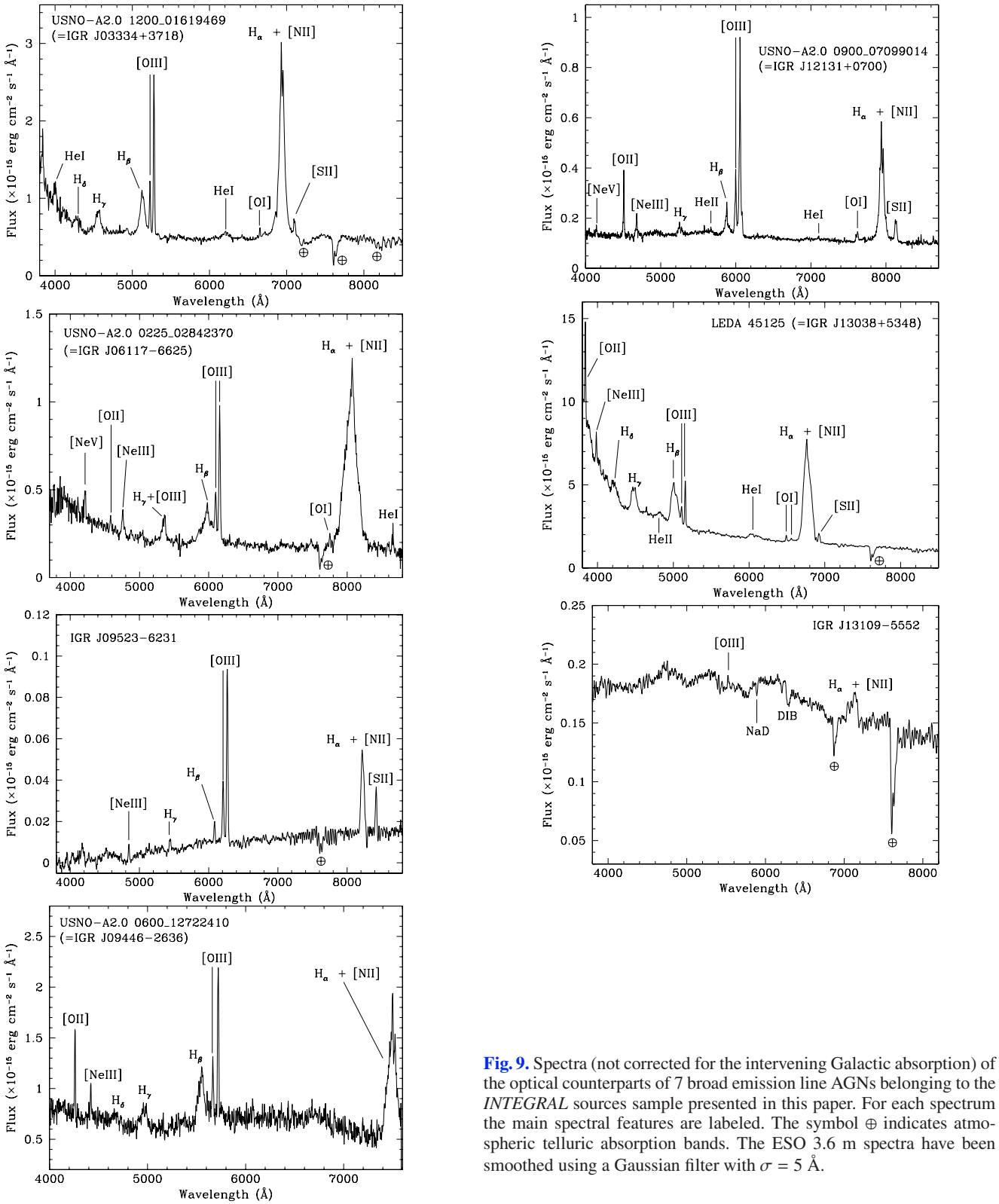

Fig. 9. Spectra (not corrected for the intervening Galactic absorption) of the optical counterparts of 7 broad emission line AGNs belonging to the *INTEGRAL* sources sample presented in this paper. For each spectrum the main spectral features are labeled. The symbol ⊕ indicates atmospheric telluric absorption bands. The ESO 3.6 m spectra have been smoothed using a Gaussian filter with σ = 5 Å.

Likewise, this latter fact suggests that XRT source #2 in the field of this source (reported by Landi et al. 2007e) marginally (if at all) contributes to the hard X-ray emission detected by IBIS as IGR J12131+0700, and it hardly is the soft X-ray counterpart of this *INTEGRAL* source.

It is noted that, for three sources (IGR J03334+3718, IGR J13038+5348 and IGR J16024−6107), the corresponding putative optical counterpart lies a few arcsecs outside the nominal *ROSAT* error circle. However, recent *Swift*/XRT pointings on the two latter sources show that their soft X-ray positions are completely consistent with the proposed optical counterparts. The same may be true for IGR J03334+3718; besides, the optical spectral appearance of its proposed counterpart strongly points to the fact that the association proposed by Burenin et al. (2006a), and studied in more detail here, is indeed correct. Similarly, the XRT and *XMM-Newton* positions for source IGR J13109−5552 are marginally consistent with each other at the 2σ level, so we consider them to be related to the same source.

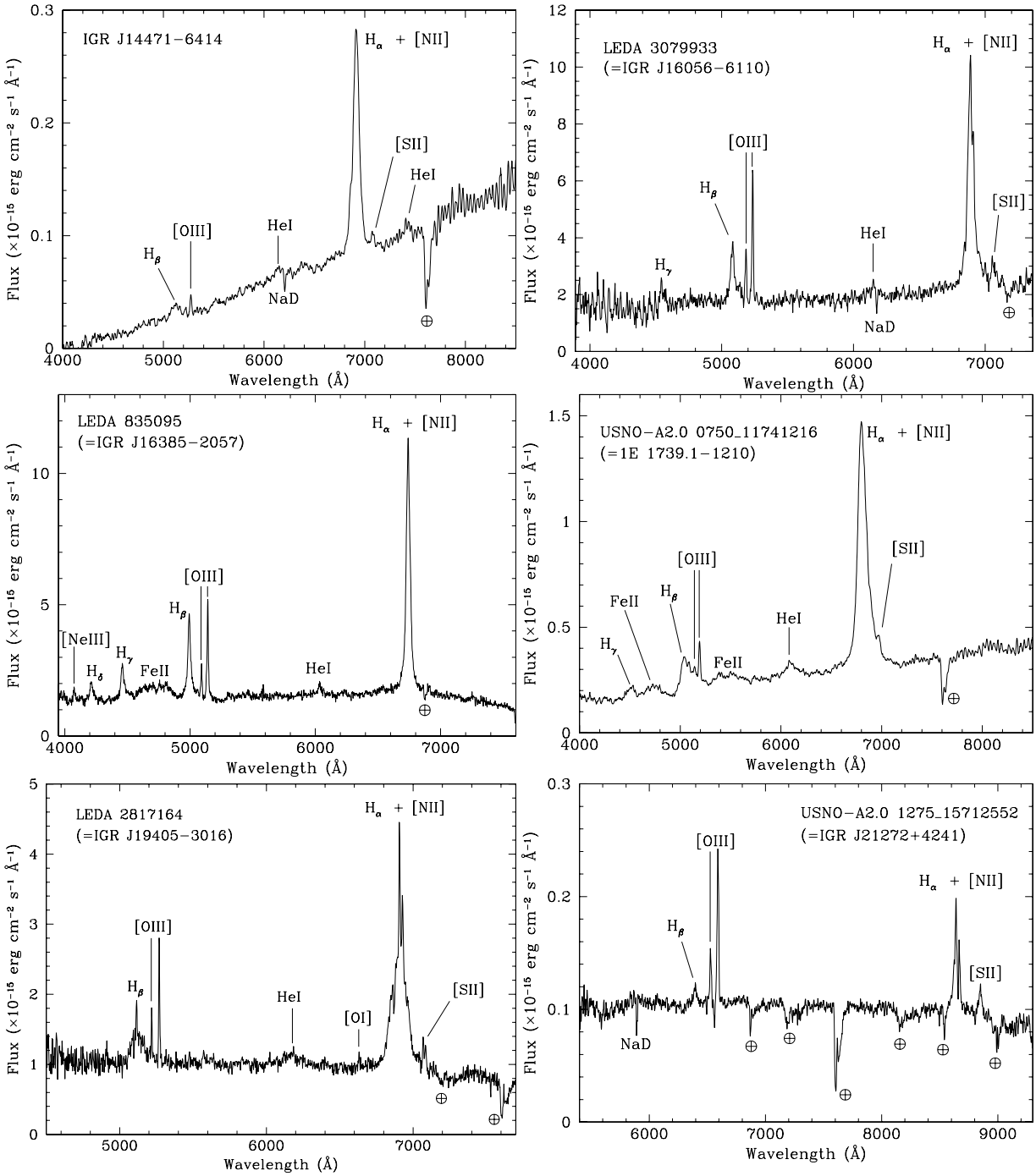

Fig. 10. Spectra (not corrected for the intervening Galactic absorption) of the optical counterparts of the remaining 6 broad emission line AGNs belonging to the *INTEGRAL* sources sample presented in this paper. For each spectrum the main spectral features are labeled. The symbol ⊕ indicates atmospheric telluric absorption bands. The ESO 3.6 m spectra have been smoothed using a Gaussian filter with σ = 5 Å.

As mentioned in Sect. 2, the putative optical counterparts of sources IGR J07437−5137 and IGR J14561−3738 were not chosen via soft X-ray catalogues cross-correlation. However, all of them are positionally consistent with a radio (NVSS or SUMSS) and a far-infrared (IRAS) source. This, despite the lack of a catalogued arcsec-sized X-ray counterpart, makes these optical objects reliable counterpart candidates for these hard X-ray sources. Indeed, the results (Landi et al. 2006, 2007a) for the three objects in Paper V without univocal arcsec-sized soft X-ray position and selected with similar criteria indicate that this approach is in any case quite successful for the selection of candidates lacking archival soft X-ray observations of the field of the corresponding hard X-ray source.

Nevertheless, we once again stress that the counterparts we propose for these sources, although likely, need confirmation through pointed soft X-ray observations with satellites capable of arcsec-sized localizations (such as *Chandra*, *XMM-Newton* or *Swift*). Keeping these caveats in mind, the above associations will be assumed to be correct in the following analysis.

Using our [O III] λ5007 line flux measurements, together with the local absorption estimate obtained from the optical spectra (see Table 6) and the 2–10 keV fluxes in Landi et al. (2007c,d), we can determine the Compton nature of Seyfert 2 AGNs IGR J00040+7020, IGR J02504+5443, IGR J11366−6002 and IGR J16024−6107 (see Bassani et al. 1999 for details on the procedure). It is found that the

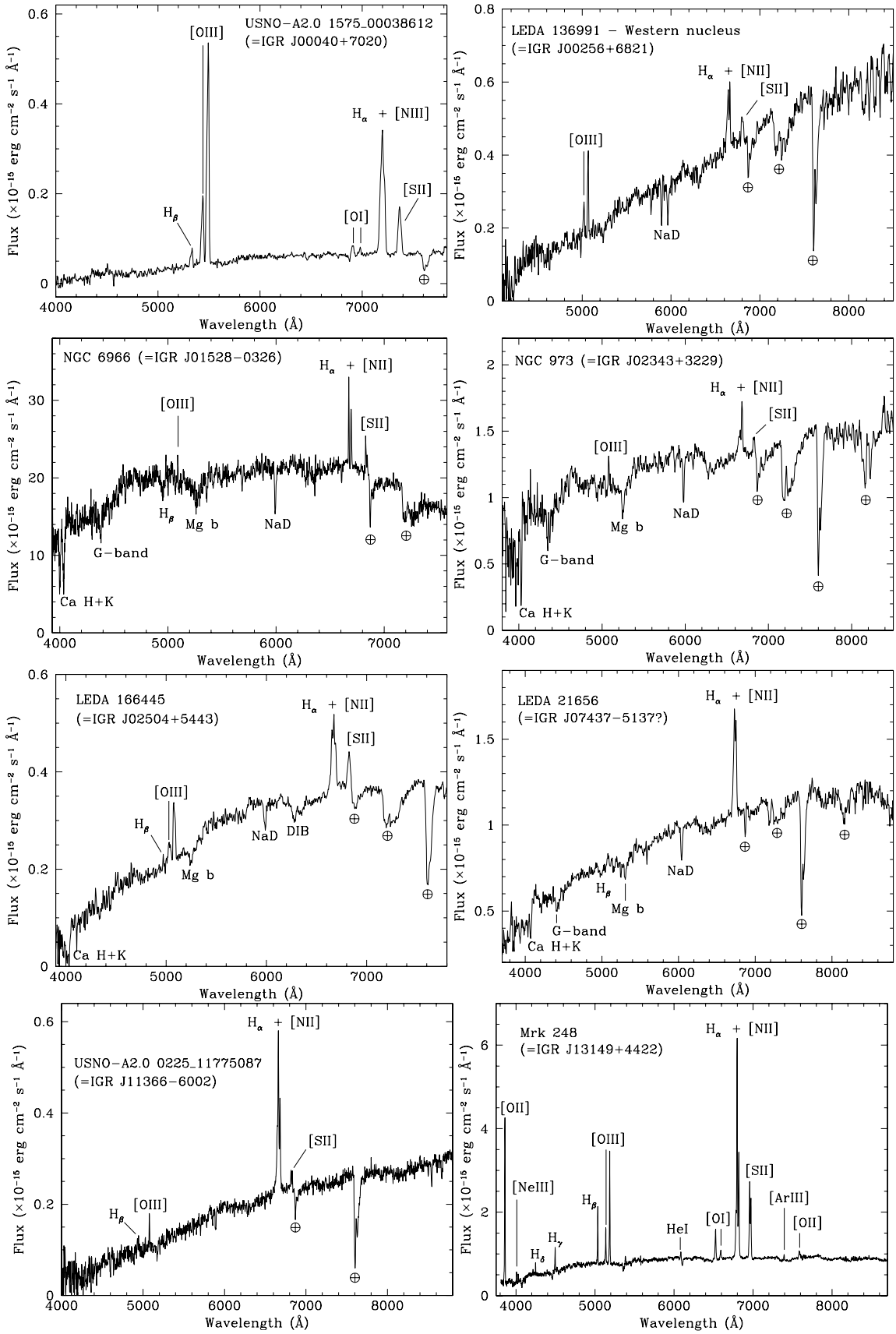

Fig. 11. Spectra (not corrected for the intervening Galactic absorption) of the optical counterparts of 8 narrow emission line AGNs belonging to the *INTEGRAL* sources sample presented in this paper. For each spectrum the main spectral features are labeled. The symbol ⊕ indicates atmospheric telluric absorption bands. The ESO 3.6 m spectra have been smoothed using a Gaussian filter with σ = 5 Å. We remark that galaxy LEDA 21656 should be considered as the tentative, although likely, counterpart of IGR J07437−5137 (see text).

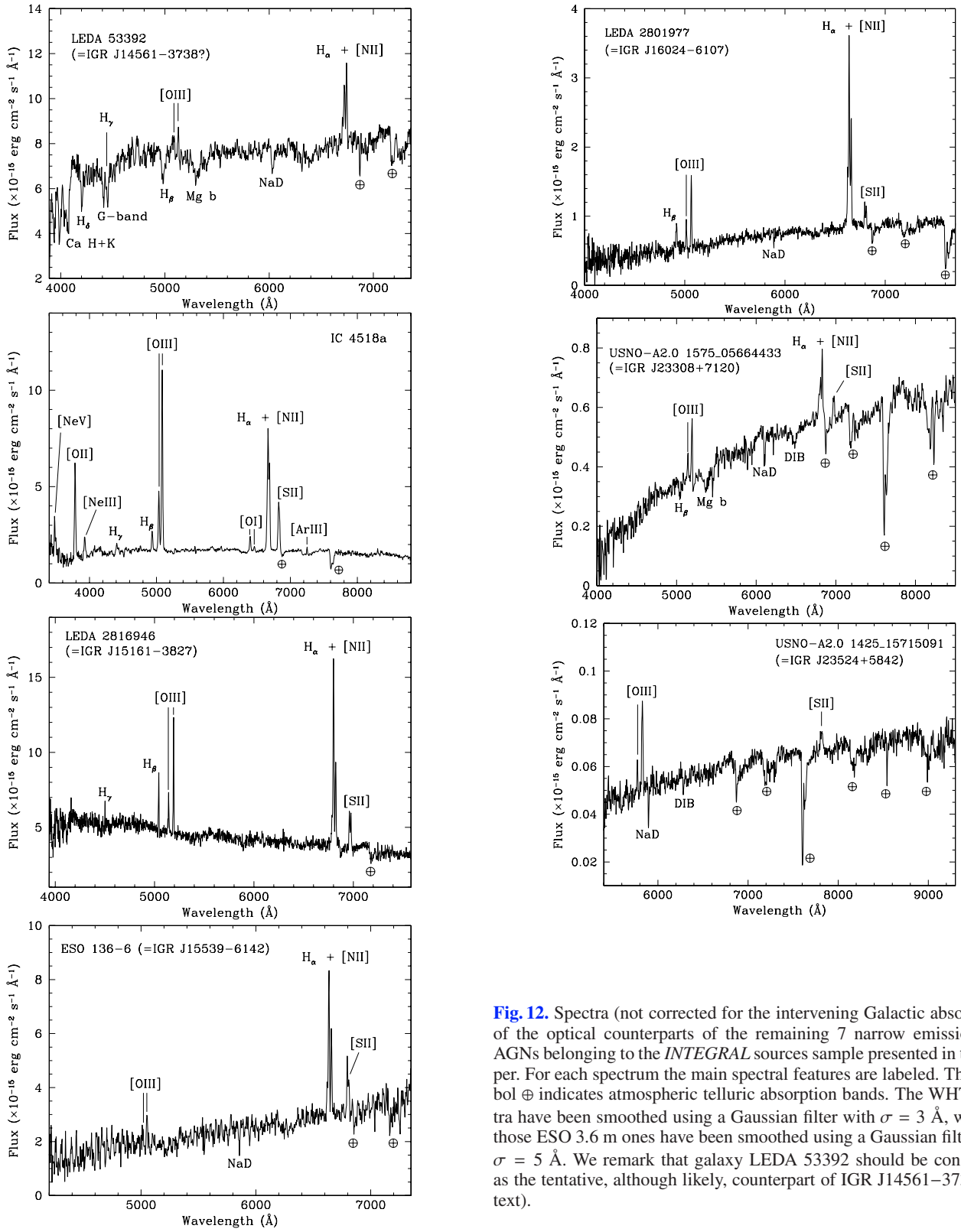

Fig. 12. Spectra (not corrected for the intervening Galactic absorption) of the optical counterparts of the remaining 7 narrow emission line AGNs belonging to the *INTEGRAL* sources sample presented in this paper. For each spectrum the main spectral features are labeled. The symbol ⊕ indicates atmospheric telluric absorption bands. The WHT spectra have been smoothed using a Gaussian filter with σ = 3 Å, whereas those ESO 3.6 m ones have been smoothed using a Gaussian filter with σ = 5 Å. We remark that galaxy LEDA 53392 should be considered as the tentative, although likely, counterpart of IGR J14561−3738 (see text).

(2–10 keV)/[O III] flux ratios of these objects range between ∼30 and ∼100: this means that all of them are Compton thin Seyfert 2 AGNs.

Likewise, for the case of Seyfert 2 AGN IGR J15161−3827, the available soft X-ray information in the 3–8 keV range (Revnivtsev et al. 2004b) allows us to say that this object has a (3–8 keV)/[O III] flux ratio of ∼9, indicating that it is a Compton thin source as well. We remark that Bassani et al. (1999) used X-ray measurements in the 2–10 keV band; therefore, the X-ray/[O III] flux ratio measure obtained for IGR J15161−3827 should be considered a strict lower limit of the actual value.

A thorough study of the soft X-ray properties of all sources of Table 6 detected below 10 keV with *Swift* and other satellites

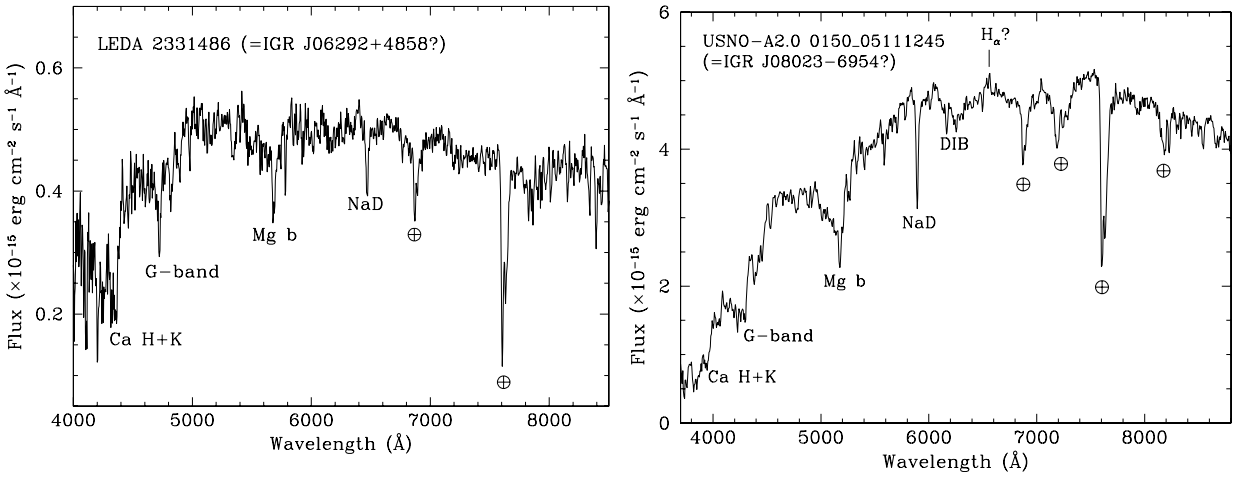

Fig. 13. Spectra (not corrected for the intervening Galactic absorption) of the optical counterparts of the two objects tentatively associated with *INTEGRAL* sources and reported in Sect. 4.4. For each spectrum the main spectral features are labeled. The symbol ⊕ indicates atmospheric telluric absorption bands.

is now underway (Landi et al., in preparation) in order to definitely determine their Compton nature.

As seen in Fig. 1, the optical counterpart of *INTEGRAL* source IGR J00256+6821 is the western nucleus of the double-nucleus galaxy LEDA 136991, as confirmed by the analysis of the optical spectrum and by the soft X-ray position afforded with *Swift*/XRT. For completeness of the information, we here report that optical spectra of the eastern nucleus, acquired simultaneously with those of the western one, indicate that both indeed lie at the same redshift; however, no trace of peculiar (emission) features are found in the eastern nucleus of LEDA 136991, thus strengthening the conclusion that only the western nucleus is responsible for the hard X-ray emission.

When one looks at Table 6, one finds that, among the Seyfert 2 AGNs for which an estimate of the local absorption can be obtained, IGR J00040+7020 seems to have no reddening local to the AGN host. This suggests that this source may be a "naked" Seyfert 2 AGN, i.e. a source which lacks the broad-line region (BLR; see, e.g., Panessa & Bassani 2002 and Bianchi et al. 2008). A low AGN accretion rate ($\lesssim 10^{-3}$: e.g., Nicastro 2000) may be the cause of an unformed BLR; in this case, given the relatively high luminosity of IGR J00040+7020, a black hole mass of $>1.2 \times 10^8$ $M_\odot$ is required, assuming an average bolometric correction (Risaliti & Elvis 2004).

Looking at the optical spectrum of the counterpart of IGR J23524+5842 we see that, at the redshift of this source, the H_α+[N II] complex regrettably falls right in the O_2 telluric band at 7605 Å, so no reliable measurements on these lines are possible. Nevertheless, the other line ratios which can be computed from this spectrum allow us to classify this source as a likely Seyfert 2 AGN.

It is also noticeable that the spectrum of IGR J13109−5552 shows a bumpy continuum which is quite anomalous for AGNs or for their host galaxies (see Figs. 9–12). A possible explanation (as already seen in Papers I and V) may be the presence of an interloping optical object in the direction of the counterpart of this X-ray source. However, the "bumpiness" of this continuum does not resemble that of any stellar spectral type. High-resolution imaging and higher S/N spectra are thus desirable to shed light on this puzzling source.

Moreover, as already mentioned, we classify IGR J16385−2057 as a NL Seyfert 1 AGN, as its optical spectrum complies with the criteria of Osterbrock & Pogge (1985) concerning the presence of the Fe II bump and the narrowness of the Full Width at Half Maximum (FWHM) of the H_β emission.

Table 7. BLR gas velocities (in km s^{-1}) and central black hole masses (in units of 10^7 $M_\odot$) for 11 Seyfert 1 AGNs belonging to the sample presented in this paper.

Object	v_{BLR}	M_{BH}
IGR J03334+3718	3600	6.2
IGR J06117−6625	8200	88
IGR J09446−2636	3700	9.7
IGR J12131+0700	3900	5.1
IGR J13038+5348	4900	5.4
IGR J14471−6414	5300	2.4
IGR J16056−6110	2200	1.9
IGR J16385−2057	1500	0.7
2E 1739.1−1210	8200	17
IGR J19405−3016	5500	62
IGR J21272+4241	1200	0.4

To conclude this section, following Wu et al. (2004) and Kaspi et al. (2000), we can compute an estimate of the mass of the central black hole in 11 of the 13 objects classified as Seyfert 1 AGN (this procedure could not be applied to IGR J09532−6231 as no broad H_β emission component was detected, and to IGR J13109−5552 because no H_β emission velocities v_{BLR} (measured from the H_β emission line FWHM) and the corresponding black hole masses for these 11 cases are reported in Table 7.

4.4. Other sources

We here report on the optical spectra of two objects tentatively identified as counterparts of two *INTEGRAL* sources, IGR J06292+4858 and IGR J08023−6954. As mentioned in Sect. 2, we consider these two identifications as tentative due to the fact that in one case (IGR J06292+4858) no arcsec-sized soft X-ray localization is available, and in the other (IGR J08023−6954) a low S/N ($\lesssim 3\sigma$) detection with *Swift/XRT* was obtained.

In the case of IGR J06292+4858, we spectroscopically observed the relatively bright ($R \sim 15.3$) galaxy LEDA 2331486 located within the IBIS error circle of this hard X-ray source. Our spectroscopy (Fig. 13, left panel) shows that the object has the characteristics of an early-type galaxy, with absorption features at redshift $z = 0.097 \pm 0.001$.

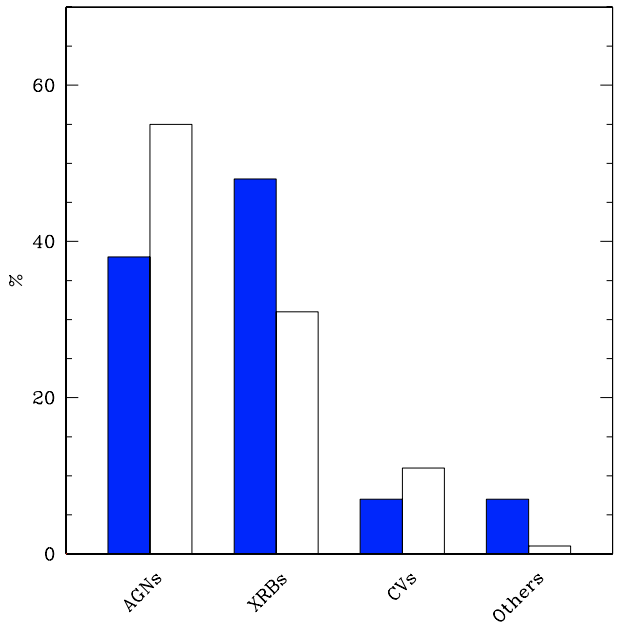

Fig. 14. Histogram, subdivided into source types, showing the percentage of *INTEGRAL* objects of known nature and belonging to the 3rd IBIS Survey (Bird et al. 2007; left-side, darker columns), and *INTEGRAL* sources from various surveys and identified through optical or NIR spectroscopy (right-side, lighter columns).

In order to better classify this source, we followed the approach of Laurent-Muehleisen et al. (1998) by using the following relevant information: (1) absence of emission lines, with an upper limit to their *EW* of ∼5 Å; (2) absence of strong Balmer absorption lines; (3) presence and strength of other absorption features (such as the G and the Mg I bands and the Ca II H+K doublet) superimposed on the galaxy continuum; (4) Ca II break contrast at 4000 Å (Br_{4000}), as defined by Dressler & Shectman (1987), with a value ∼40%. All of the above suggests that this galaxy can be tentatively classified as a possible BL Lac object. If indeed IGR J06292+4858 and LEDA 2331486 are the same object, we obtain 20–40 keV and 40–100 keV luminosities of 1.8×10^{45} erg s^{-1} and $<1.6 \times 10^{45}$ erg s^{-1}, assuming a luminosity distance d_L = 479.9 Mpc and the fluxes reported in Bird et al. (2007).

Concerning IGR J08023−6954, the optical spectrum of its putative optical counterpart, star USNO-A2.0 0150_05111245 (Fig. 13, right panel) shows the continuum typical of a late-G/early-K star, with the presence of a weak H_α emission at $z = 0$, with flux $(4.2 \pm 0.8) \times 10^{-15}$ erg cm^{-2} s^{-1} and EW = 0.86±0.17 Å. This suggests a chromospherically active star identification (e.g., an RS CVn type system) for this source if the low S/N XRT detection is indeed real.

Of course, deeper multiwavelegth followup is needed to confirm (or disprove) the two tentative identifications above.

4.5. Statistical considerations

We can now briefly update the statistical approach made in Paper V by including the results presented here, along with recent identifications of *INTEGRAL* sources as HMXBs (Hannikainen et al. 2007; Leyder et al. 2007; Masetti et al. 2007h), LMXBs (Masetti et al. 2007c) and AGNs (Bassani et al. 2007; Masetti et al. 2008).

It is found that, presently, of the 97 *INTEGRAL* sources identified through optical or NIR spectroscopy, 55 (57%) are AGNs (almost equally divided into Seyfert 1 s and Seyfert 2 s), 30 (31%) are X-ray binaries (with a large majority, i.e. more than 86%, of HMXBs), and 11 (11%) are CVs, with 8 of them definitely or likely belonging to the IP subclass (see Papers IV, V and the present work) and 3 of symbiotic star type.

One can compare (see Fig. 14), for instance, these percentages with those of the 308 identified objects belonging to the largest catalogue of *INTEGRAL* sources published up to now, i.e., the 3rd IBIS Survey (Bird et al. 2007). In this survey we have 147 (48%) X-ray binaries (about half of which are HMXBs), 118 (38%) AGNs and 23 (7%) CVs, with most (perhaps all) of them of magnetic nature (IPs or Polars; see Barlow et al. 2006).

These numbers confirm once more the effectiveness of this method of catalogue cross-correlation plus optical spectroscopy followup in revealing the AGN and CV nature of a large number of unidentified *INTEGRAL* sources, while it may introduces a bias against detecting X-ray binaries: this is however quite understandable, given that, as *INTEGRAL* is sensitive to the hard X-ray radiation, it can easily detect sources deeply embedded in the Galactic Plane dust and therefore heavily obscured (as already stressed by, e.g., Walter 2007). Thus, we foresee that the use of NIR spectroscopy followup will reveal a larger number of absorbed X-ray binaries.

We conclude by remarking that, of the 97 optical and NIR spectroscopic identifications mentioned here, 78 were obtained within the framework of our spectroscopic follow-up program (Papers I–V, the present work, and references therein).

5. Conclusions

In our continuing effort of identification of *INTEGRAL* sources by means of optical spectroscopy (Papers I–V), we have identified and studied 39 hard X-ray objects of unknown or poorly explored nature by means of a multisite campaign at 8 different telescopes and using the archival data of 2 spectroscopic surveys.

We found that the selected sample is made of 29 AGNs (13 of which are of Seyfert 1 type, 15 are Seyfert 2 AGNs and 1 is possibly a BL Lac), 5 HMXBs, 2 LMXBs, 1 magnetic CV, 1 symbiotic star and 1 active star. In terms of relative sizes of these groups, we notice the overwhelming majority (74%) of AGNs in the present sample.

We recall that, in four cases (IGR J06292+4858, IGR J07437−5137, IGR J08023−6954 and IGR J14561−3738), only a tentative albeit likely optical counterpart was given because of the lack of a definite arcsec-sized soft X-ray position. Thus, for them an observation with sufficient S/N to be achieved using soft X-ray satellites affording arcsec-sized localizations (such as *Chandra*, *XMM-Newton* or *Swift*) is needed to confirm the proposed association.

The results presented in this work further indicate the high effectiveness of this method of catalogue cross-correlation plus optical spectroscopy to pinpoint the nature of the still unidentified *INTEGRAL* sources. We now plan to extend this approach to NIR spectroscopy.

Acknowledgements. We thank Silvia Galleti for Service Mode observations at the Loiano telescope; Hripsime Navasardyan for Service Mode observations at the Asiago Telescope; Don Pollacco and Neil Mahoney for Service Mode observations at the WHT; Stefano Bernabei, Ivan Bruni, Antonio De Blasi and Roberto Gualandi for night assistance at the Loiano telescope; Claudio Aguilera, Arturo Gómez, Edgardo Cosgrove and Alberto Miranda for day and night assistance at the CTIO telescope; Antonio De Franceschi for night assistance at CASLEO; Gaspare Lo Curto and Alessandro Ederoclite for the support at the

ESO telescopes; Ariel Sánchez and Andrés González for night assistance at the ESO 3.6 m telescope. We also thank the anonymous referee for useful remarks which helped us to improve the paper. This research has made use of the ASI Science Data Center Multimission Archive; it also used the NASA Astrophysics Data System Abstract Service, the NASA/IPAC Extragalactic Database (NED), and the NASA/IPAC Infrared Science Archive, which are operated by the Jet Propulsion Laboratory, California Institute of Technology, under contract with the National Aeronautics and Space Administration. This publication made use of data products from the Two Micron All Sky Survey (2MASS), which is a joint project of the University of Massachusetts and the Infrared Processing and Analysis Center/California Institute of Technology, funded by the National Aeronautics and Space Administration and the National Science Foundation. This research has also made use of data extracted from the 6dF Galaxy Survey and the Sloan Digitized Sky Survey archives; it has also made use of the ESO Science Archive operated at Garching bei München, Germany, of the SIMBAD database operated at CDS, Strasbourg, France, and of the HyperLeda catalogue operated at the Observatoire de Lyon, France. The authors acknowledge the ASI and INAF financial support via grant No. I/023/05/0. N.M. and S.A.C. were Visiting Astronomers at CASLEO, operated under agreement between the Consejo Nacional de Investigaciones Científicas y Técnicas de la República Argentina and the National Universities of La Plata, Córdoba and San Juan. The CCD and data acquisition system at CASLEO have been partly financed by R. M. Rich through US NSF grant AST-90-15827. G.E.R. and S.A.C. were supported by grants PICT 03-13291 BID 1728/OC-AR (ANPCyT), PIP 5375 (CONICET), and AYA2007-68034-C03-01 (FEDER funds). L.M. is supported by the University of Padua through grant No. CPDR061795/06. N.M. thanks ESO for the pleasant hospitality in Santiago de Chile during the preparation of this paper.

References

Adelman-McCarthy, J. K., Agüeros, M. A., Allam, S. S., et al. 2007, ApJS, 172, 634
Barlow, E. J., Knigge, C., Bird, A. J., et al. 2006, MNRAS, 372, 224
Bassani, L., Dadina, M., Maiolino, R., et al. 1999, ApJS, 121, 473
Bassani, L., Landi, R., Malizia, A., et al. 2007, ApJ, 669, L1
Bianchi, S., Corral, A., Panessa, F., et al. 2008, MNRAS, 385, 195
Bird, A. J., Malizia, A., Bazzano, A., et al. 2007, ApJS, 170, 175
Bodaghee, A., Courvoisier, T. J.-L., Rodriguez, J., et al. 2007, A&A, 467, 585
Bonnet-Bidaud, J. M., de Martino, D., Falanga, M., et al. 2007, A&A, 473, 185
Burenin, R., Mescheryakov, A., Revnivtsev, M., et al. 2006a, ATel 880
Burenin, R., Mescheryakov, A., Sazonov, S., et al. 2006b, ATel, 883
Cardelli, J. A., Clayton, G. C., & Mathis, J. S. 1989, ApJ, 345, 245
Chaty, S. 2007, ChJAA, in press [arXiv:0710.0292]
Condon, J. J., Cotton, W. D., Greisen, E. W., et al. 1998, AJ, 115, 1693
Corbet, R. H. D. 1986, MNRAS, 220, 1047
Doyle, M. T., Drinkwater, M. J., Rohde, D. J., et al. 2005, MNRAS, 361, 34
Dressler, A., & Shectman, S. 1987, AJ, 94, 899
Ducati, J. R., Bevilacqua, C. M., Rembold, S. B., & Ribeiro, D. 2001, ApJ, 558, 309
Gros, A., Goldwurm, A., Cadolle-Bel, M., et al. 2003, A&A, 411, L179
Gunn, J. E., & Stryker, L. L. 1983, ApJS, 52, 121
Halpern, J. P. 2006, ATel, 847
Hannikainen, D. C., Rawlings, M. G., Muhli, P., et al. 2007, MNRAS, 380, 665
Harris, D. E., Forman, W., Gioia, I. M., et al. 1994, SAO HEAD CD-ROM Series I (Einstein), Nos. 18–36
Hill, A. B., Walter, R., Knigge, C., et al. 2005, A&A, 439, 255
Ho, L. C., Filippenko, A. V., & Sargent, W. L. W. 1993, ApJ, 417, 63
Ho, L. C., Filippenko, A. V., & Sargent, W. L. W. 1997, ApJS, 112, 315
in 't Zand J., Jonker, P., Méndez, M., & Markwardt, C. 2006, ATel 915
IRAS 1988, The Point Source Catalog, version 2.0, NASA RP-1190
Jacoby, G. H., Hunter, D. A., & Christian, C. A. 1984, ApJS, 56, 257
Jones, D. H., Saunders, W., Colless, M., et al. 2004, MNRAS, 355, 747
Jones, D. H., Saunders, W., Read, M., & Colless, M. 2005, PASA, 22, 277
Kaspi, S., Smith, P. S., Netzer, H., et al. 2000, ApJ, 533, 631
Kauffmann, G., Heckman, T. M., Tremonti, C., et al. 2003, MNRAS, 346, 1055
Keek, S., Kuiper, L., & Hermsen, W. 2006, ATel 810
Krivonos, R., Revnivtsev, M., Lutovinov, A., et al. 2007, A&A, 475, 775
Kuiper, L., den Hartog, P. R., & Hermsen, W. 2006, ATel 939
Landi, R., Masetti, N., Gehrels, N., et al. 2006, ATel 945
Landi, R., Masetti, N., Gehrels, N., et al. 2007a, ATel 990
Landi, R., Masetti, N., Bassani, L., et al. 2007b, ATel 1273
Landi, R., Malizia, A., Masetti, N., et al. 2007c, ATel 1274
Landi, R., Masetti, N., Stephen, J. B., et al. 2007d, ATel 1288
Landi, R., Malizia, A., Masetti, N., et al. 2007e, ATel 1310
Landi, R., Masetti, N., Sguera, V., et al. 2007f, ATel 1322
Lang, K. R. 1992, Astrophysical Data: Planets and Stars (New York: Springer-Verlag)
Laurent-Muehleisen, S. A., Kollgaard, R. I., Ciardullo, R., et al. 1998, ApJS, 118, 127
Leitherer, C. 1988, ApJ, 326, 356
Leyder, J.-C., Walter, R., Lazos, M., et al. 2007, A&A, 465, L35
Masetti, N., Palazzi, E., Bassani, L., et al. 2004, A&A, 426, L41 (Paper I)
Masetti, N., Mason, E., Bassani, L., et al. 2006a, A&A, 448, 547 (Paper II)
Masetti, N., Pretorius, M. L., Palazzi, E., et al. 2006b, A&A, 449, 1139 (Paper III)
Masetti, N., Bassani, L., Bazzano, A., et al. 2006c, A&A, 455, 11 (Paper IV)
Masetti, N., Morelli, L., Palazzi, E., et al. 2006d, A&A, 459, 21 (Paper V)
Masetti, N., Bassani, L., Malizia, A., Bird, A. J., & Ubertini, P. 2006e, ATel, 941
Masetti, N., Malizia, A., Dean, A. J., Bazzano, A., & Walter, R. 2006f, ATel, 957
Masetti, N., Bassani, L., Bazzano, A., et al. 2006h, ATel 815
Masetti, N., Morelli, L., Cellone, S. A., et al. 2007a, ATel, 1033
Masetti, N., Cellone, S. A., Landi, R., et al. 2007b, ATel 1034
Masetti, N., Landi, R., Pretorius, M. L., et al. 2007c, A&A, 470, 331
Masetti, N., Mason, E., Landi, R., et al., 2008, A&A, 480, 715
Mauch, T., Murphy, T., Buttery, H. J., et al. 2003, MNRAS, 342, 1117
Negueruela, I., & Smith, D. M. 2006, ATel, 831
Negueruela, I., Smith, D. M., Torrejón J.M, & Reig, P. 2007, Supergiant Fast X-ray Transients: A common behaviour or a class of objects?, in The 6th INTEGRAL Workshop - The Obscured Universe, ed. S. Grebenev, S. A. Sunyaev, & C. Winkler (Noordwijk: ESA Publication Division), ESA-SP 622, 255
Nicastro, F. 2000, ApJ, 530, L65
Osterbrock, D. E. 1989, Astrophysics of Gaseous Nebulae and Active Galactic Nuclei (Mill Valley: Univ. Science Books)
Osterbrock, D. E., & Pogge, R. W. 1985, ApJ, 297, 166
Panessa, F., & Bassani, L. 2002, A&A, 394, 435
Predehl, P., & Schmitt, J. H. M. M. 1995, A&A, 293, 889
Prugniel, P. 2005, The Hyperleda Catalogue, http://leda.univ-lyon1.fr
Revnivtsev, M., Sunyaev, R. A., Varshalovich, D. A., et al. 2004a, Astron. Lett., 30, 382
Revnivtsev, M., Sazonov, S., Jahoda, K., & Gilfanov, M. 2004b, A&A, 418, 927
Risaliti, G., & Elvis, M. 2004, A Panchromatic View of AGN, in Supermassive Black Holes in the Distant Universe, ed. A. J. Barger, Astrophysics and Space Science Library (Dordrecht: Kluwer Academic Publishers), 308, 187
Rodriguez, J., Tomsick, J. A., & Chaty, S. 2008, A&A, in press [arXiv:0712.1005]
Saxton R. D., Read, A. M., Esquej, P., et al. 2008, A&A, 480, 611
Schlegel, D. J., Finkbeiner, D. P., & Davis, M. 1998, ApJ, 500, 525
Skrutskie, M. F., Cutri, R. M., Stiening, R., et al. 2006, AJ, 131, 1163
Sguera, V., Bazzano, A., Bird, A. J., et al. 2006, ApJ, 646, 452
Sguera, V., Hill, A. B., Bird, A. J., et al. 2007, A&A, 467, 249
Stephen, J. B., Bassani, L., Molina, M., et al. 2005, A&A, 432, L49
Stephen, J. B., Bassani, L., Malizia, A., et al. 2006, A&A, 445, 869
Torres, M. A. P., Garcia, M. R., McClintock, J. E., et al. 2004, ATel 264
Ubertini, P., Lebrun, F., Di Cocco, G., et al. 2003, A&A, 411, L131
van Paradijs, J., & McClintock, J. E. 1995, Optical and ultraviolet observations of X-ray binaries, in: X-ray Binaries, ed. W. H. G. Lewin, J. van Paradijs, & E. P. J. van den Heuvel (Cambridge: Cambridge University Press), 58
Veilleux, S., & Osterbrock, D. E. 1987, ApJS, 63, 295
Voges, W., Aschenbach, B., Boller, T., et al. 1999, A&A, 349, 389
Walter, R. 2007, Ap. Space Sci., 309, 5
Walter, R., Courvoisier, T. J.-L., Foschini, L., et al. 2004, IGR J16318−4848 & Co.: a new population of hidden high-mass X-ray binaries in the Norma Arm of the Galaxy, in: Procs. of the Fifth INTEGRAL Workshop, ed. B. Battrick, V. Schoenfelder, G. Lichti, & C. Winkler (Noordwijk: ESA Publication Division), ESA-SP 552, 417
Walter, R., Zurita Heras, J., Bassani, L., et al. 2006, A&A, 453, 133
Warner, B. 1995, Cataclysmic variable stars (Cambridge: Cambridge University Press)
Wegner, W. 1994, MNRAS, 270, 229
Winkler, H. 1992, MNRAS, 257, 677
Winkler, C., Courvoisier, T. J.-L., Di Cocco, G., et al. 2003, A&A, 411, L1
Wright, E. L. 2006, PASP, 118, 1711
Wu, X.-B., Wang, R., Kong, M. Z., Liu, F. K., & Han, J. L. 2004, A&A, 424, 793